

Two Categories of Approximately μ - τ Symmetric Neutrino Mass Textures

Kenichi Fuki*

*Department of Physics, Tokyo Metropolitan University,
1-1 Minami-Osawa, Hachioji, Tokyo 192-0397, Japan*

Masaki Yasue†

*Department of Physics, Tokai University,
1117 Kitakaname, Hiratsuka,
Kanagawa 259-1292, Japan
(Dated: August, 2006)*

Our approximately μ - τ symmetric neutrino mass textures fall into two different categories, whose behaviors in the μ - τ symmetric limit are characterized by either $\sin \theta_{13} \rightarrow 0$ (referred to as C1)), or $\sin \theta_{12} \rightarrow 0$ (referred to as C2)), where θ_{12} and θ_{13} , respectively stand for the ν_e - ν_μ and ν_e - ν_τ mixing angles. We present ten phenomenologically viable neutrino mass textures: two for the normal mass hierarchy, three for the inverted mass hierarchy, and five for the quasi degenerate mass pattern. Tiny μ - τ symmetry breaking ensures that $\sin^2 \theta_{13} \ll 1$ for C1), and $\Delta m_\odot^2 / \Delta m_{atm}^2 (\equiv R) \ll 1$ for C2), where $\Delta m_\odot^2 = m_2^2 - m_1^2$ for solar neutrinos, and $\Delta m_{atm}^2 = |m_3^2 - (m_1^2 + m_2^2)/2|$ for atmospheric neutrinos with $m_{1,2,3}$ being neutrino masses. A correlation among small quantities is provided by $\cos 2\theta_{23} \sim \sin \theta_{13}$ for C1), and by either $\cos 2\theta_{23} \sim R$, or $\cos 2\theta_{23} \sin \theta_{13} \sim R$ for C2), where θ_{23} is the ν_μ - ν_τ mixing angle. It is further shown that $\tan 2\theta_{12} \sim \cos 2\theta_{23} / \sin \theta_{13}$ is satisfied for C2). We find the following properties for each mass ordering: 1) For the normal mass hierarchy, the other smallness of R (or $\sin^2 \theta_{13}$) in the case of C1) (or C2)) can be ascribed to an approximate electron number conservation; 2) For the normal and inverted mass hierarchies and for the quasi degenerate mass pattern II (with $m_{1,2,3}^2 \gg \Delta m_{atm}^2$) exhibiting $m_1 \sim m_2 \sim m_3$, all in the case of C2), either $R \sim \tan 2\theta_{12} \sin^2 \theta_{13}$ or $R \sim \tan 2\theta_{12} \sin \theta_{13}$ is satisfied; 3) For the inverted mass hierarchy and the quasi degenerate mass pattern I (with $|m_{1,2,3}| \sim \sqrt{\Delta m_{atm}^2}$), both in the case of C1) with $m_1 \sim -m_2$, the relation $R \sim \sin^2 \theta_{13}$ arises from the contribution of $\mathcal{O}(\sin^2 \theta_{13})$ in the estimation of neutrino masses; and 4) For the quasi degenerate mass pattern II, we observe that $m_{\beta\beta}$ can be as large as 0.5 eV, where $m_{\beta\beta}$ is the effective neutrino mass in $(\beta\beta)_{0\nu}$ -decay, and that larger values of $m_{\beta\beta}$ favor larger values of $\sin \theta_{13}$ in the case of C1) for $m_1 \sim m_2 \sim m_3$ and smaller values of $\sin \theta_{13}$ in the cases of C1) for $m_1 \sim m_2 \sim -m_3$ and C2) for $m_1 \sim m_2 \sim \pm m_3$.

PACS numbers: 12.60.-i, 13.15.+g, 14.60.Pq, 14.60.St

I. INTRODUCTION

Neutrinos are massive particles [1], which undergo neutrino oscillations that have been first confirmed to exist for atmospheric neutrinos by the Super-Kamiokande collaboration [2]. The similar neutrino oscillations [3] have also been observed in neutrinos from the Sun [4, 5], from accelerators [6], and from reactors [7]. Masses of such neutrinos, which are much lighter than the electron mass, can be created by theoretical mechanisms such as the seesaw mechanism [8, 9], and the radiative mechanism [10, 11]. The oscillations are interpreted as a result of the mixings among three flavor neutrinos ν_e , ν_μ , and ν_τ , which are converted into three massive neutrinos ν_1 , ν_2 , and ν_3 during their flight. Their masses $m_{1,2,3}$ and mixing angles $\theta_{12,23,13}$ are currently constrained to be [12]:

$$\Delta m_\odot^2 = 7.92 (1 \pm 0.09) \times 10^{-5} \text{ eV}^2, \quad \Delta m_{atm}^2 = 2.4 \left(1^{+0.21}_{-0.26} \right) \times 10^{-3} \text{ eV}^2, \quad (1)$$

where Δm_\odot^2 , and Δm_{atm}^2 are neutrino mass differences squared given by $\Delta m_\odot^2 = m_2^2 - m_1^2$ (> 0 [13]) for solar neutrinos, and $\Delta m_{atm}^2 = |m_3^2 - (m_1^2 + m_2^2)/2|$ for atmospheric neutrinos, and

$$\sin^2 \theta_{12} = 0.314 \left(1^{+0.18}_{-0.15} \right), \quad \sin^2 \theta_{23} = 0.44 \left(1^{+0.41}_{-0.22} \right), \quad \sin^2 \theta_{13} = \left(0.9^{+2.3}_{-0.9} \right) \times 10^{-2}. \quad (2)$$

*Electronic address: fuki@phys.metro-u.ac.jp

†Electronic address: yasue@keyaki.cc.u-tokai.ac.jp

These mixing angles parameterize the PMNS unitary matrix U_{PMNS} [1] to give

$$U_{PMNS} = \begin{pmatrix} c_{12}c_{13} & s_{12}c_{13} & s_{13} \\ -s_{12}c_{23} - c_{12}s_{23}s_{13} & c_{12}c_{23} - s_{12}s_{23}s_{13} & s_{23}c_{13} \\ s_{12}s_{23} - c_{12}c_{23}s_{13} & -c_{12}s_{23} - s_{12}c_{23}s_{13} & c_{23}c_{13} \end{pmatrix}, \quad (3)$$

which transforms ν_f ($f = e, \mu, \tau$) into ν_i ($i = 1, 2, 3$): $\nu_f = (U_{PMNS})_{fi}\nu_i$, where $c_{ij} \equiv \cos\theta_{ij}$, and $s_{ij} \equiv \sin\theta_{ij}$. Two distinct properties are present in these observed data [14]. One is that the mixing angle θ_{13} is suppressed to show $\sin^2\theta_{13} \ll 1$ but the atmospheric, and solar mixing angles $\theta_{12,23}$ are not suppressed, and satisfy $\sin^2 2\theta_{12,23} = \mathcal{O}(1)$. The other is that Δm_{\odot}^2 , and Δm_{atm}^2 show the hierarchy $\Delta m_{\odot}^2/\Delta m_{atm}^2 \ll 1$. These properties may provide a great hint on how the underlying neutrino physics looks like.

It has been argued that the μ - τ symmetry, which is based on the invariance of flavor neutrino mass terms under the interchange of ν_{μ} , and ν_{τ} [15, 16, 17, 18, 19], well describes the suppression of $\sin^2\theta_{13} \ll 1$ as well as the large mixings of $\sin^2 2\theta_{12,23} = \mathcal{O}(1)$. The suppression reflects the fact that this symmetry requires $\sin\theta_{13} = 0$ and its tiny breaking induces $\sin\theta_{13} \ll 1$. To obtain the hierarchy $\Delta m_{\odot}^2/\Delta m_{atm}^2 \ll 1$ may need an additional assumption such as that of the approximate conservation of the electron number [20, 21]. As another consequence of the tiny breaking of the μ - τ symmetry, we have discussed in Ref.[22] that the hierarchy $\Delta m_{\odot}^2/\Delta m_{atm}^2 \ll 1$ can appear instead of the suppression of $\sin^2\theta_{13} \ll 1$. In this case, we obtain $\sin\theta_{12} \rightarrow 0$ (referred to as C2)) instead of $\sin\theta_{13} \rightarrow 0$ (referred to as C1)) in the μ - τ symmetric limit.¹ In both cases, we have found that $\cos 2\theta_{23}$ vanishes in the μ - τ symmetric limit. Therefore, $\cos 2\theta_{23}$ is a good measure of the μ - τ symmetry breaking. To obtain $\sin^2 2\theta_{12} = \mathcal{O}(1)$ from $\sin\theta_{12} \sim \varepsilon$ in C2), where ε represents the μ - τ symmetry breaking parameter, we have to introduce another small parameter denoted by η to cancel ε . In fact, the mixing angle θ_{12} is determined to be $\tan 2\theta_{12} \sim \varepsilon/\eta$, leading to $\sin^2 2\theta_{12} = \mathcal{O}(1)$ if $\eta \sim \varepsilon$ while it vanishes as $\varepsilon \rightarrow 0$ for a fixed η . Namely, we find that $\tan 2\theta_{12} \sim \cos 2\theta_{23}/\sin\theta_{13}$. Any textures in C2) must be constrained so as to appropriately contain this small factor η .

Useful relations among $\sin^2\theta_{13}$, $\Delta m_{\odot}^2/\Delta m_{atm}^2$, and $\cos 2\theta_{23}$ [24, 25] have been derived on the general ground [22], where we rely upon the μ - τ symmetry breaking but not on details of textures. Namely, we have found that $\cos 2\theta_{23} \sim \sin\theta_{13}$ for C1), and $\cos 2\theta_{23} \sim R$ for C2). It is also discussed in Ref.[22] that the hierarchy $\Delta m_{\odot}^2/\Delta m_{atm}^2 \ll 1$ in C1) can be accounted for by the relation $\Delta m_{\odot}^2/\Delta m_{atm}^2 \sim \sin^2\theta_{13}$ induced by effects of $\mathcal{O}(\sin^2\theta_{13})$ appearing in the estimation of neutrino masses. This relation is specific to textures with $m_1 + m_2 \sim 0$ [26] and is found to be satisfied by the inverted mass hierarchy, and the quasi degenerate mass pattern with $|m_{1,2,3}| \sim \sqrt{\Delta m_{atm}^2}$. On the other hand, in C2), because of $\tan 2\theta_{12} \sim \cos 2\theta_{23}/\sin\theta_{13}$, it turns out that $\Delta m_{\odot}^2/\Delta m_{atm}^2 \sim \tan 2\theta_{12} \sin^2\theta_{13}$ and $\Delta m_{\odot}^2/\Delta m_{atm}^2 \sim \tan 2\theta_{12} \sin\theta_{13}$ are, respectively, satisfied for the normal and inverted mass hierarchies.

It is known that the μ - τ symmetry is badly broken by the charged leptons. Since the neutrinos and charged leptons form the $SU(2)_L$ -doublets, the assumed μ - τ symmetry for neutrinos may not be well preserved. This fact apparently disfavors the requirement of the μ - τ symmetry. However, if neutrinos are Majorana particles, it is theoretically possible to have an approximate μ - τ symmetry for neutrinos but not for charged leptons who are Dirac particles. This difference can supply approximately μ - τ symmetric flavor structure for neutrinos and the dominance of Type II seesaw mechanism [9] is thus preferred [27]. There are several examples to have the μ - τ symmetry for neutrinos [17, 19, 28, 29]. One way to reconcile with the difficulty is to introduce a few Higgs scalars with, say, different Z_2 parity, or other different quantum numbers associated with extra symmetries that can discriminate among various Higgs scalars, where their vevs can provide charged lepton masses in such a way that the charged leptons acquire almost diagonal masses. In this case, there necessarily arise flavor-changing neutral current interactions due to the direct exchanges of these Higgs scalars. Such effects become sizable for quarks when quarks and leptons are unified and should be suppressed.

In this article, we construct phenomenologically viable neutrino mass textures in our categories C1), and C2) that account for the present observed properties of neutrino oscillations. There are ten textures: two of them provide the normal mass hierarchy, other three of them provide the inverted mass hierarchy, and the remaining five of them provide the quasi degenerate mass pattern. Among five textures for the quasi degenerate mass pattern, one textures for C1) describe neutrinos with $|m_{1,2,3}| \sim \sqrt{\Delta m_{atm}^2}$ [26, 30, 31]. To estimate neutrino masses, and mixings, we use general formula shown in the Appendix A, where terms of $\mathcal{O}(\sin^2\theta_{13})$ are property taken into account to see that $\Delta m_{\odot}^2/\Delta m_{atm}^2 \sim \sin^2\theta_{13}$ is naturally realized in some of textures for C1). In the next section, we review what was derived in Ref.[22]. In Sec.III, we present ten textures, where the general relations obtained in Sec.II are found to be indeed satisfied. In the quasi degenerate mass pattern with $m_{1,2,3}^2 \gg \Delta m_{atm}^2$, the effective neutrino mass in $(\beta\beta)_{0\nu}$ -decay is shown to be as large as 0.5 eV [32]. The final section Sec.IV is devoted to summary, and discussions.

¹ The possible choice of $\sin\theta_{12} = 0$ has also been mentioned in Ref.[23].

II. NEUTRINO MASSES AND MIXING ANGLES UP TO $\mathcal{O}(\sin^2 \theta_{13})$

Our neutrino mass matrix M_ν is parameterized by the sum of the μ - τ symmetric part M_{sym} , and the symmetry breaking part M_b :² $M_\nu = M_{sum} + M_b$ with

$$M_{sym} = \begin{pmatrix} a & b & -\sigma b \\ b & d & e \\ -\sigma b & e & d \end{pmatrix}, \quad M_b = \varepsilon \begin{pmatrix} 0 & b' & \sigma b' \\ b' & d' & 0 \\ \sigma b' & 0 & -d' \end{pmatrix}, \quad (4)$$

where ε stands for a tiny μ - τ symmetry breaking parameter. We focus on clarifying flavor structure of M_ν to see how large or small each flavor neutrino mass is, and calculate neutrino masses, and mixing angles directly from M_ν in the normal mass hierarchy, the inverted mass hierarchy, and the quasi degenerate mass pattern.³ Various flavor structures consistent with the observed data to be obtained in the next section are visually analyzed.

There is a simple reason why Eq.(4) leads to either $\sin \theta_{13} = 0$ or $\sin \theta_{12} = 0$. One of the eigenvectors for M_{sym} is given by $(0, \sigma/\sqrt{2}, 1/\sqrt{2})^T$. It supplies a column vector placed in U_{PMNS} , which can be either $(s_{13}, s_{23}c_{13}, c_{23}c_{13})^T$ or $(s_{12}c_{13}, c_{12}c_{23} - s_{12}s_{23}s_{13}, -c_{12}s_{23} - s_{12}c_{23}s_{13})^T$ depending on the ordering of the eigenvalues. By comparing our eigenvector with one of these two column vectors, we obtain that

$$\tan 2\theta_{12} = \frac{2\sqrt{2}b}{d - \sigma e - a}, \quad \tan 2\theta_{23} = \sigma, \quad \sin \theta_{13} = 0, \quad (5)$$

for $(s_{13}, s_{23}c_{13}, c_{23}c_{13})^T$, and

$$\sin \theta_{12} = 0, \quad \tan 2\theta_{23} = -\sigma, \quad \tan 2\theta_{13} = -\frac{2\sqrt{2}\sigma b}{d - \sigma e - a}, \quad (6)$$

for $(s_{12}c_{13}, c_{12}c_{23} - s_{12}s_{23}s_{13}, -c_{12}s_{23} - s_{12}c_{23}s_{13})^T$, where $(0, 1/\sqrt{2}, \sigma/\sqrt{2})^T$ is used instead of $(0, \sigma/\sqrt{2}, 1/\sqrt{2})^T$.

Since the μ - τ symmetry breaking generally induces the deviation of the atmospheric neutrino mixing from the maximal one, we parameterize this deviation by Δ :

$$c_{23} = \frac{1 + \Delta}{\sqrt{2(1 + \Delta^2)}}, \quad s_{23} = \pm \sigma \frac{1 - \Delta}{\sqrt{2(1 + \Delta^2)}}, \quad (7)$$

giving $\sin 2\theta_{23} = \pm \sigma(1 - \Delta^2)/(1 + \Delta^2)$, and $\cos 2\theta_{23} = 2\Delta/(1 + \Delta^2)$. The plus (minus) sign in s_{23} corresponds to the sign for $\tan 2\theta_{23}$ in Eq.(5) (Eq.(6)). The estimation of the masses and the mixing angles is summarized in the Appendix A, where corrections of $\mathcal{O}(\sin^2 \theta_{13})$ are included. It should be noted that this estimation does not recourse to the conventional perturbative expansions which provide order by order construction of eigen values (for masses) and eigen vectors (for mixing angles) because we know the exact expressions of masses and mixing angles given by Eqs.(A2)-(A5) in the Appendix A.

The suppression of Δm_\odot^2 is obviously possible if either

$$m_1 + m_2 \sim 0, \text{ or } m_1 - m_2 \sim 0, \quad (8)$$

is satisfied. This trivial condition can give useful relations when m_1 and m_2 calculated in the Appendix A are used. Namely, the mass difference $m_1 - m_2$ is connected to the quantity X defined in Eq.(A6). In C2), the smallness of X is a direct consequence of the tiny μ - τ symmetry breaking as can be seen from Eq.(A14). Since Δm_\odot^2 is expressed in terms of X as

$$\Delta m_\odot^2 = \frac{2\sqrt{2}(m_1 + m_2)X}{\sin 2\theta_{12}}, \quad (9)$$

the appearance of $\Delta m_\odot^2/\Delta m_{atm}^2 \ll 1$ is a natural result in C2). On the other hand, in C1), since X is not necessarily suppressed, the appearance of $\Delta m_\odot^2/\Delta m_{atm}^2 \ll 1$ is not a natural result. We have to suppress X unless the condition $m_1 + m_2 \sim 0$ is satisfied.

² It is understood that the charged leptons, and neutrinos are rotated, if necessary, to give diagonal charged-current interactions, and to define the flavor neutrinos of ν_e , ν_μ , and ν_τ .

³ See Ref.[33] for indirect discussions on the approximately μ - τ symmetric flavor neutrino masses, which utilize the mass eigenstates instead of the flavor eigenstates.

The additional requirements are present in C1) and C2). First, in C1), we may require that

$$d - \sigma e + a = 0, \quad (10)$$

to realize $m_1 + m_2 \sim 0$ in Eq.(A9). More precisely, we demand that $|d - \sigma e + a| \lesssim \varepsilon^2$. If this is the case, we find that

$$\frac{\Delta m_{\odot}^2}{\Delta m_{atm}^2} \sim \sin^2 \theta_{13}, \quad (11)$$

which arises from textures with $m_2 \approx -m_1 \approx \sqrt{2}X/\sin 2\theta_{12}$ and $m_3 \sim d + e\sigma$

- for the inverted mass hierarchy if $d + e\sigma \sim 0$, giving $|m_3| \sim \sin^2 \theta_{13} |m_{1,2}|$;
- for the quasi degenerate mass pattern if $|d + e\sigma| \sim |X/\sin 2\theta_{12}|$, giving $|m_{1,2,3}| \sim \sqrt{\Delta m_{atm}^2}$.

These two mass patterns in C1) allow $\Delta m_{\odot}^2/\Delta m_{atm}^2$ to correlate with $\sin^2 \theta_{13}$. The relation Eq.(11) has been already derived in Ref.[24, 25], but our reason for the appearance of this relation is a purely perturbative one focusing on the effects of $\mathcal{O}(\sin^2 \theta_{13})$ [22, 30].

Next, in C2), there are two constraints, which guarantee that $\sin^2 \theta_{13} \ll 1$ and $\sin^2 2\theta_{12} = \mathcal{O}(1)$. For $\sin^2 \theta_{13} \ll 1$, we need $Y \sim 0$ because $\tan 2\theta_{13} \propto Y$ in Eq.(A13). Since Y is mainly determined by b , the μ - τ symmetric mass, we must realize $b \sim 0$. For $\sin^2 2\theta_{12} = \mathcal{O}(1)$, we require that $|d + \sigma e - a| \propto |\varepsilon|$ in Eq.(A13) leading to $\tan 2\theta_{12} \propto X/\varepsilon$ only if X cancels the effect from ε in the denominator to yield $\tan 2\theta_{12} = \mathcal{O}(1)$. Therefore, we must realize that

$$b \sim 0, \quad |d + \sigma e - a| \propto |\varepsilon|, \quad (12)$$

in C2). Hereafter, to suppress the contribution from b , another small parameter denoted by η presumably of $\mathcal{O}(\varepsilon)$ is introduced.

III. NEUTRINO MASS HIERARCHY

In this section, neutrino mass textures, which describe the present observed patterns of neutrino masses and mixings, are constructed. We present ten textures, two for the normal mass hierarchy, three for the inverted mass hierarchy, one for the quasi degenerate mass pattern I (with $|m_{1,2,3}| \sim \sqrt{\Delta m_{atm}^2}$) and four for the quasi degenerate mass pattern II (with $m_{1,2,3}^2 \gg \Delta m_{atm}^2$).⁴ Since we would like to see the effects from $\sin^2 \theta_{13}$ in $\Delta m_{\odot}^2/\Delta m_{atm}^2$, we calculate, in the Appendix A, all the quantities up to $\mathcal{O}(\varepsilon^2)$, where the terms of $\mathcal{O}(\varepsilon^2)$ are responsible for $\Delta m_{\odot}^2/\Delta m_{atm}^2 \ll 1$ in some textures.

To construct textures, we consider general constraints on the flavor neutrino masses found in Sec.II. First, the constraint from Eq.(8) to obtain $\Delta m_{\odot}^2/\Delta m_{atm}^2 \ll 1$ is satisfied in various mass patterns. Namely, we require

- for the normal mass hierarchy with $m_{1,2}^2 \sim 0 (\ll m_3^2)$, $X \sim 0$ in Eq.(13) for C1), and Eq.(20) for C2);
- for the inverted mass hierarchy with $m_{1,2}^2 \gg m_3^2$, either $X \sim 0$ in Eq.(29) for C1), and Eq.(47) for C2), or $m_2 + m_1 \sim 0$ in Eq.(34) for C1);
- for the quasi degenerate mass pattern I with $|m_{1,2,3}| \sim \sqrt{\Delta m_{atm}^2}$, $m_1 + m_2 \sim 0$ in Eq.(55) for C1);
- for the quasi degenerate mass pattern II with $m_{1,2,3}^2 \gg \Delta m_{atm}^2$, $X \sim 0$ in Eqs.(69) and (86) for C1), and Eqs.(76) and (95) for C2).

Furthermore, we can realize $\Delta m_{\odot}^2/\Delta m_{atm}^2 \sim \sin^2 \theta_{13}$ for C1) if we choose

- for the inverted mass hierarchy with $m_1 + m_2 \sim 0$, $d + \sigma e \sim 0$ to give $m_3 \sim 0$;
- for the quasi degenerate mass pattern I with $m_1 + m_2 \sim 0$, $|d + \sigma e| \sim |\sqrt{2}X/\sin 2\theta_{12}|$ to give $m_3 \sim |m_{1,2}|$.

Finally, for C2), we find that Eq.(12) to obtain $\tan 2\theta_{12} = \mathcal{O}(1)$ is satisfied in such a way that

⁴ See Ref.[24], where some of the results are shared.

- for the normal mass hierarchy, $d + \sigma e \sim 0$ and $a \sim 0$ are imposed;
- for the inverted mass hierarchy, $d + \sigma e \sim a (\neq 0)$ is imposed;
- for the quasi degenerate mass pattern II with $m_{1,2} \sim m_3$, $d \sim a (\neq 0)$ and $e \sim 0$
- for the quasi degenerate mass pattern II with $m_{1,2} \sim -m_3$, $d \sim 0$ and $e \sim \sigma a$ are imposed.

The predictions from these textures are plotted in FIG.1-FIG.15 for $\tan 2\theta_{12} > 0$ and $\sigma = 1$, where $|\varepsilon| \leq 1/3$ is taken to satisfy $\varepsilon^2 \lesssim 0.1$. The results from $\tan 2\theta_{12} < 0$ are covered by the changes of the signs of other parameters, and all figures are depicted as functions of $|\sin \theta_{13}|$, where the difference in the sign of σ becomes irrelevant. No constraint on the range of η is applied but we find that η is phenomenologically bounded to satisfy $\eta^2 \ll 1$ because η is linked to either $\Delta m_{\odot}^2 / \Delta m_{atm}^2$, or $\sin \theta_{13}$. All calculations to show our scattered plots are based on the formula shown in the Appendix A, which are derived by the approximation due to $\varepsilon^2 \ll 1$ but not due to $\eta^2 \ll 1$. The approximation due to $\eta^2 \ll 1$ is solely used to show compact forms of calculate masses and mixing angles in terms of the flavor neutrino masses in order to explain behaviors of the scattered plots. There are additional parameters of $\mathcal{O}(1)$, p for M_{ee} , q for $M_{e\mu, e\tau}$, r and r' for $M_{\mu\mu, \tau\tau}$, and s for $M_{\mu\tau}$, whose magnitudes run from $1/3$ to 3 to show the scattered plots.

A. Normal Mass Hierarchy

1. Category C1) with $s_{23} \sim \sigma/\sqrt{2}$

The mass ordering is given by $m_1^2 < m_2^2 \ll m_3^2$, which is realized by

$$M_{\nu}^{C1)} = d_0 \begin{pmatrix} p\eta & \eta + \varepsilon & -\sigma(\eta - \varepsilon) \\ \eta + \varepsilon & 1 + r'\varepsilon & \sigma(1 - s\eta) \\ -\sigma(\eta - \varepsilon) & \sigma(1 - s\eta) & 1 - r'\varepsilon \end{pmatrix}. \quad (13)$$

From the texture, neutrino masses are predicted to be:

$$\begin{aligned} m_1 &\approx \left(\frac{2(p+s)\eta - (2+r'^2)\varepsilon^2}{4} - \frac{2\eta - r'\varepsilon^2}{\sqrt{2}\sin 2\theta_{12}} \right) d_0, \\ m_2 &\approx \left(\frac{2(p+s)\eta - (2+r'^2)\varepsilon^2}{4} + \frac{2\eta - r'\varepsilon^2}{\sqrt{2}\sin 2\theta_{12}} \right) d_0, \\ m_3 &\approx \frac{2(2-s\eta) + (2+r'^2)\varepsilon^2}{2} d_0, \end{aligned} \quad (14)$$

and

$$\Delta m_{\odot}^2 \approx \frac{[2(p+s)\eta - (2+r'^2)\varepsilon^2](2\eta + r'\varepsilon^2)}{\sqrt{2}\sin 2\theta_{12}} d_0^2, \quad \Delta m_{atm}^2 \approx 4d_0^2, \quad (15)$$

and mixing angles are calculated to be

$$\tan 2\theta_{12} \approx \frac{2\sqrt{2}(2\eta - r'\varepsilon^2)}{2(s-p)\eta + (2-r'^2)\varepsilon^2}, \quad \tan 2\theta_{13} \approx \sqrt{2}\sigma\varepsilon, \quad \cos 2\theta_{23} \approx -r'\varepsilon. \quad (16)$$

This texture utilizes both $X \approx 0$ and $m_1 + m_2 \approx 0$ to have $\Delta m_{\odot}^2 / \Delta m_{atm}^2 \ll 1$. As a result, $|\eta| \gg \varepsilon^2$ is preferred because, for $|\eta| \lesssim \varepsilon^2$, $\Delta m_{\odot}^2 / \Delta m_{atm}^2 \sim \varepsilon^4 \sim \sin^4 \theta_{13}$, which is experimentally too small to account for the observed size of $\Delta m_{\odot}^2 / \Delta m_{atm}^2$. It is thus expected that

$$\eta \sim \sqrt{\frac{\Delta m_{\odot}^2}{\Delta m_{atm}^2}}, \quad (17)$$

is satisfied. There is a simple relation between θ_{13} , and θ_{23} , which is

$$\cos 2\theta_{23} \approx -\sqrt{2}\sigma r' \sin \theta_{13}. \quad (18)$$

It should be noted that p can be neglected in these predictions and that the smallness of p can be ascribed to the approximate electron number (L_e) conservation [20, 21]. Suppose that the L_e -conservation is violated by tiny $|\Delta L_e| = 1$ interactions [20], which are characterized by the strength η , then, it is reasonable to expect the relation

$$M_{ee} : M_{ei} : M_{ij} \sim \eta^2 : \eta : 1, \quad (19)$$

to arises, where $i, j = \mu, \tau$. The smallness of $\Delta m_\odot^2 / \Delta m_{atm}^2$ is a result of tiny breaking of the electron number conservation.

The predictions $\Delta m_\odot^2 / \Delta m_{atm}^2$ and $\cos 2\theta_{23}$ are plotted in FIG.1-C1) and FIG. 2-C1) as functions of $|\sin \theta_{13}|$. Since there is no efficient constraint on the region of η arising from $|\eta| \gtrsim \varepsilon^2$,

- $\Delta m_\odot^2 / \Delta m_{atm}^2 (\sim \eta^2)$ can have values for all ranges of $\sin \theta_{13} (\sim \varepsilon)$

as in FIG.1-C1). For $\cos 2\theta_{13}$, the proportionality of $\cos 2\theta_{23}$ to $\sin \theta_{13}$ in Eq.(18) indicates that

- two straight boundaries for $\cos 2\theta_{23} > 0$ or $\cos 2\theta_{23} < 0$ correspond to $|\cos 2\theta_{23}| \sim 3\sqrt{2}|\sin \theta_{13}|$ and $|\cos 2\theta_{23}| \sim \sqrt{2}|\sin \theta_{13}|/3$ from $1/3 \leq |r'| \leq 3$, and
- the forbidden region near $\cos 2\theta_{23} = 0$ shows up for $\sin \theta_{13} \neq 0$

as in FIG.2-C1). Since p can vanish, the figures have been produced by adopting $|p| \leq 3$ instead of $1/3 \leq |p| \leq 3$.

2. Category C2) with $s_{23} \sim -\sigma/\sqrt{2}$

We also find the similar texture with $\sigma \rightarrow -\sigma$ in the μ - τ entry of Eq.(13). To obtain $\sin^2 \theta_{13} \ll 1$, b must be suppressed and the texture indeed provides extra suppression due to η . The texture is given by

$$M_\nu^{C2)} = d_0 \begin{pmatrix} p\eta & \eta + \varepsilon & -\sigma(\eta - \varepsilon) \\ \eta + \varepsilon & 1 + r'\varepsilon & -\sigma(1 - s\eta) \\ -\sigma(\eta - \varepsilon) & -\sigma(1 - s\eta) & 1 - r'\varepsilon \end{pmatrix}. \quad (20)$$

The masses are calculated to be:

$$\begin{aligned} m_1 &\approx \left(\frac{2(p+s)\eta - r'^2\varepsilon^2}{4} - \frac{\sqrt{2}\varepsilon}{\sin 2\theta_{12}} \right) d_0, & m_1 &\approx \left(\frac{2(p+s)\eta - r'^2\varepsilon^2}{4} + \frac{\sqrt{2}\varepsilon}{\sin 2\theta_{12}} \right) d_0, \\ m_3 &\approx \frac{2(2-s\eta) + r'^2\varepsilon^2}{2} d_0, \end{aligned} \quad (21)$$

and

$$\Delta m_\odot^2 \approx \frac{\sqrt{2}[2(p+s)\eta - r'^2\varepsilon^2]\varepsilon}{\sin 2\theta_{12}}, \quad \Delta m_{atm}^2 \approx 4d_0^2, \quad (22)$$

and mixing angles are

$$\tan 2\theta_{12} \approx \frac{4\sqrt{2}\varepsilon}{2(s-p)\eta - r'^2\varepsilon^2}, \quad \tan 2\theta_{13} \approx -\sqrt{2}\sigma\eta, \quad \cos 2\theta_{23} \approx -r'\varepsilon. \quad (23)$$

There is also the possibility to have the approximate electron number conservation that accounts for the smallness of η , which in turn ensures the smallness of $\sin \theta_{13}$. To obtain $\tan 2\theta_{12} = \mathcal{O}(1)$, we require that $|\eta| \gg \varepsilon^2$ suggesting $|\eta| \sim |\varepsilon|$.

Since the terms proportional to ε^2 can be neglected, we find that

$$\cos 2\theta_{23} \approx \frac{\sigma(s-p)r'\tan 2\theta_{12}}{2} \sin \theta_{13}. \quad (24)$$

This relation suggests that

$$\tan 2\theta_{12} \sim \frac{\cos 2\theta_{23}}{\sin \theta_{13}}, \quad (25)$$

which is specific to the category C2). There is another correlation

$$\frac{\Delta m_{\odot}^2}{\Delta m_{atm}^2} \approx \frac{\sigma(s+p)}{r' \sin 2\theta_{12}} \cos 2\theta_{23} \sin \theta_{13}, \quad (26)$$

where $\Delta m_{\odot}^2/\Delta m_{atm}^2 \sim \eta\varepsilon$ from Eq.(22). These two relations give

$$\frac{\Delta m_{\odot}^2}{\Delta m_{atm}^2} \approx \frac{s^2 - p^2}{2 \cos 2\theta_{12}} \sin^2 \theta_{13}. \quad (27)$$

In this texture,

$$\frac{\Delta m_{\odot}^2}{\Delta m_{atm}^2} \sim \sin^2 \theta_{13}, \quad (28)$$

is realized.

The predictions $\Delta m_{\odot}^2/\Delta m_{atm}^2$ and $\cos 2\theta_{23}$ are depicted in FIG.1-C2) and FIG.2-C2) as functions of $|\sin \theta_{13}|$, where $|p| \leq 3$ is also used to include the case of $p = 0$. In these figures, we find that

- $|\sin \theta_{13}| \gtrsim 0.06$ because of Eq.(28),

which requires that $|\sin \theta_{13}| \sim 0.1$. Because of $\varepsilon \neq 0$ for $\tan 2\theta_{12} \neq 0$,

- $\cos 2\theta_{23}$ is not allowed to vanish

as shown in FIG.2-C2).

B. Inverted Mass Hierarchy

1. Category C1) with $s_{23} \sim \sigma/\sqrt{2}$

The mass ordering is given by $m_3^2 \ll m_1^2 < m_2^2$. There are two types depending on the relative sign of m_1 , and m_2 . The first texture gives $m_1 \sim m_2$, and takes the form of

$$M_{\nu}^{C1)} = d_0 \begin{pmatrix} 2 - p\eta & \eta + \varepsilon & -\sigma(\eta - \varepsilon) \\ \eta + \varepsilon & 1 + r'\varepsilon & -\sigma(1 - s\eta) \\ -\sigma(\eta - \varepsilon) & -\sigma(1 - s\eta) & 1 - r'\varepsilon \end{pmatrix}. \quad (29)$$

Neutrino masses are predicted to be:

$$\begin{aligned} m_1 &\approx \left(2 - \frac{2(p+s)\eta - (2+r'^2)\varepsilon^2}{4} - \frac{2\eta + r'\varepsilon^2}{\sqrt{2} \sin 2\theta_{12}} \right) d_0, \\ m_2 &\approx \left(2 - \frac{2(p+s)\eta - (2+r'^2)\varepsilon^2}{4} + \frac{2\eta + r'\varepsilon^2}{\sqrt{2} \sin 2\theta_{12}} \right) d_0, \\ m_3 &\approx \left(s\eta - \frac{2+r'^2}{2}\varepsilon^2 \right) d_0, \end{aligned} \quad (30)$$

and

$$\Delta m_{\odot} \approx \frac{4\sqrt{2}(2\eta + r'\varepsilon^2)}{\sin 2\theta_{12}} d_0^2, \quad \Delta m_{atm}^2 \approx 4d_0^2, \quad (31)$$

and mixing angles are

$$\tan 2\theta_{12} \approx \frac{2\sqrt{2}(2\eta + r'\varepsilon^2)}{2(p-s)\eta - (2-r'^2)\varepsilon^2}, \quad \tan 2\theta_{13} \approx -\sqrt{2}\sigma\varepsilon, \quad \cos 2\theta_{23} \approx r'\varepsilon. \quad (32)$$

In this texture, we also have

$$\cos 2\theta_{23} \approx -\sqrt{2}\sigma r' \sin \theta_{13}, \quad (33)$$

as in C1) for the normal mass hierarchy. From the expression of $\tan 2\theta_{12}$, no a priori constraint on η arises because both η and ε^2 are present in the denominator and numerator.⁵ To realize $\Delta m_{\odot}^2/\Delta m_{atm}^2 = \mathcal{O}(0.01)$, $|2\eta + r'\varepsilon^2|$ should be $\mathcal{O}(0.01)$. The predictions $\Delta m_{\odot}^2/\Delta m_{atm}^2$ and $\cos 2\theta_{23}$ are depicted in FIG.3-C1) and FIG.4-C1) as functions of $|\sin \theta_{13}|$. These predictions give similar dependences of $\sin \theta_{13}$ to those in C1) for the normal mass hierarchy. The proportionality of $\cos 2\theta_{23}$ to $\sin \theta_{13}$ also yields the straight boundaries in FIG.4-C1).

The next texture is characterized by $m_1 \sim -m_2$, and is given by

$$M_{\nu}^{C1)} = d_0 \begin{pmatrix} -(2-\eta) & q+\varepsilon & -\sigma(q-\varepsilon) \\ q+\varepsilon & 1+r'\varepsilon & -\sigma \\ -\sigma(q-\varepsilon) & -\sigma & 1-r'\varepsilon \end{pmatrix}. \quad (34)$$

Neutrino masses are predicted to be

$$\begin{aligned} m_1 &\approx - \left(\frac{\sqrt{2}q}{\sin 2\theta_{12}} - \frac{\eta - 2[t_{13}^2 + (\Delta - \varepsilon r')\Delta]}{2} \right) d_0, \\ m_2 &\approx \left(\frac{\sqrt{2}q}{\sin 2\theta_{12}} + \frac{\eta - 2[t_{13}^2 + (\Delta - \varepsilon r')\Delta]}{2} \right) d_0, \\ m_3 &\approx 2(t_{13}^2 + (\Delta - \varepsilon r')\Delta) d_0, \end{aligned} \quad (35)$$

and

$$\Delta m_{\odot}^2 \approx \frac{2\sqrt{2}q[\eta - 2(t_{13}^2 + (\Delta - \varepsilon r')\Delta)]}{\sin 2\theta_{12}} d_0^2, \quad \Delta m_{atm}^2 \approx \frac{2q^2 d_0^2}{\sin^2 2\theta_{12}}, \quad (36)$$

and mixing angles are

$$\tan 2\theta_{12} \approx \frac{q}{\sqrt{2}}, \quad \tan 2\theta_{13} \approx \sqrt{2}\sigma \frac{2 - qr'}{2 + q^2} \varepsilon, \quad \cos 2\theta_{23} \approx 2\Delta, \quad (37)$$

where

$$\Delta = \frac{r' + q}{2 + q^2} \varepsilon. \quad (38)$$

Since we have $\tan 2\theta_{12} > 0$, we know that $q > 0$ and $q \sim 3$ to yield $\sin^2 2\theta_{12} \sim 0.8$.

We find that

$$\cos 2\theta_{23} \approx \frac{\sqrt{2}\sigma(r' + q)}{2 - qr'} \sin \theta_{13}. \quad (39)$$

For $r' > 0$, it just gives the proportionality of $\cos 2\theta_{23}$ to $\sin \theta_{13}$ for the fixed values of q and r' because $r' + q$ in the coefficient of Δ does not vanish. On the other hand, for $r' < 0$, $\cos 2\theta_{23}$ can vanish. For $|\eta| \gg \varepsilon^2$, we find that

$$\Delta m_{\odot}^2 \approx \frac{4\eta}{\cos 2\theta_{12}} d_0^2, \quad \eta \sim \frac{\Delta m_{\odot}^2}{\Delta m_{atm}^2}. \quad (40)$$

For the opposite case, we may choose $\eta = 0$. The mass hierarchy is taken care of by $\varepsilon^2 \sim \sin^2 \theta_{13}$ and Δm_{\odot}^2 becomes

$$\Delta m_{\odot}^2 \approx - \frac{4\sqrt{2}q[t_{13}^2 + (\Delta - \varepsilon r')\Delta]}{\sin 2\theta_{12}} d_0^2, \quad (41)$$

which is converted into

$$\Delta m_{\odot}^2 \approx \frac{2\sqrt{2}q}{\sin 2\theta_{12}} \left[\frac{(r' + q)^2}{2 + q^2} - 1 \right] \varepsilon^2. \quad (42)$$

⁵ Unlike in the normal mass hierarchy case, we obtain $\Delta m_{\odot}^2/\Delta m_{atm}^2 \sim \varepsilon^2 \sim \sin^2 \theta_{13}$, which is the right order of $\Delta m_{\odot}^2/\Delta m_{atm}^2$. This possibility will be discussed elsewhere.

The constraint to obtain $\Delta m_\odot^2 > 0$ can be satisfied if $r' < -\sqrt{2+q^2} - q$ or $r' > \sqrt{2+q^2} - q$, which gives $r' \geq 1/3$ because $1/3 \leq |r'| \leq 3$ and $q \sim 3$. For $r' \geq 1/3$,

$$\frac{\Delta m_\odot^2}{\Delta m_{atm}^2} \approx \sin^2 \theta_{13} \quad (43)$$

is satisfied and $|\cos 2\theta_{23}| \sim |\sin \theta_{13}|$ is expected.

Shown in FIG.5, and FIG.6 are the predictions of $\Delta m_\odot^2/\Delta m_{atm}^2$, and $\cos 2\theta_{23}$ as functions of $|\sin \theta_{13}|$. To enhance the relationship of Eq.(43), we use two regions: one with $|\eta| > 0.001$ and the other $|\eta| \leq 0.001$ in the figures. In the region with $|\eta| \leq 0.001$, η is hard to saturate the size of $\Delta m_\odot^2/\Delta m_{atm}^2$, which is $\mathcal{O}(0.01)$; therefore, $\Delta m_\odot^2/\Delta m_{atm}^2$ should be determined by $\sin^2 \theta_{13}$. It is understood that FIG.6 for $|\eta| > 0.001$ is produced by two contributions: one from $r' > 0$ marked by the black dots and the other from $r' < 0$ marked by the grey dots. Namely,

- for $r' > 0$ giving $r' + q \neq 0$, the straight boundaries appear because of $\cos 2\theta_{23} \propto \sin \theta_{13}$, and
- for $r' < 0$ giving $r' + q \sim 0$, $\cos 2\theta_{23} \sim 0$ is allowed,

as suggested by Eq.(39). In these figures,

- the contribution that gives $\Delta m_\odot^2/\Delta m_{atm}^2 \approx \sin^2 \theta_{13}$ does manifest themselves for $|\eta| \leq 0.001$,

which constrains $|\sin \theta_{13}|$ to be $\mathcal{O}(0.1)$. From FIG.6 for $|\eta| \leq 0.001$, we find that this texture with $\eta \sim 0$ can describes $\Delta m_\odot^2/\Delta m_{atm}^2 \approx \sin^2 \theta_{13}$ with

$$0.02 \lesssim |\sin \theta_{13}| \lesssim 0.10, \text{ and } -0.25 \lesssim \cos 2\theta_{23} \lesssim -0.18, \text{ or } 0.18 \lesssim \cos 2\theta_{23} \lesssim 0.30, \quad (44)$$

where the range of $|\cos 2\theta_{23}|$ is in accord with Eq.(39).

For $\eta = 0$, if we choose $q = 3$ leading to $\sin^2 2\theta_{12} = 9/11$, and $r' = 2$, we obtain

$$\sin \theta_{13} \approx -\frac{2\sqrt{2}\sigma\varepsilon}{11}, \quad \cos 2\theta_{23} \approx \frac{10\varepsilon}{11}, \quad \Delta m_\odot^2 \approx 12d_0^2\varepsilon^2, \quad \Delta m_{atm}^2 \approx 22d_0^2, \quad (45)$$

which give

$$\frac{\Delta m_\odot^2}{\Delta m_{atm}^2} \approx 8 \sin^2 \theta_{13}. \quad (46)$$

To be consistent with the observation of $\Delta m_\odot^2/\Delta m_{atm}^2$, we find that $0.06 \lesssim |\sin \theta_{13}| \lesssim 0.07$.

2. Category C2) with $s_{23} \sim -\sigma/\sqrt{2}$

There is only one texture that can explain the observed results. The texture yields $m_1 \sim m_2$ and takes the following form:

$$M_\nu^{C2)} = d_0 \begin{pmatrix} 2 - p\eta & \eta + \varepsilon & -\sigma(\eta - \varepsilon) \\ \eta + \varepsilon & 1 + r'\varepsilon & \sigma(1 - s\eta) \\ -\sigma(\eta - \varepsilon) & \sigma(1 - s\eta) & 1 - r'\varepsilon \end{pmatrix}. \quad (47)$$

The masses are calculated to be:

$$\begin{aligned} m_1 &\approx \left(2 - \frac{2(p+s)\eta - r'^2\varepsilon^2}{4} - \frac{\sqrt{2}\varepsilon}{\sin 2\theta_{12}} \right) d_0, & m_2 &\approx \left(2 - \frac{2(p+s)\eta - r'^2\varepsilon^2}{4} + \frac{\sqrt{2}\varepsilon}{\sin 2\theta_{12}} \right) d_0, \\ m_3 &\approx \left(s\eta - \frac{r'^2}{2}\varepsilon^2 \right) d_0, \end{aligned} \quad (48)$$

and

$$\Delta m_\odot^2 \approx \frac{8\sqrt{2}\varepsilon d_0^2}{\sin 2\theta_{12}}, \quad \Delta m_{atm}^2 \approx 4d_0^2, \quad (49)$$

and mixing angles are

$$\tan 2\theta_{12} \approx \frac{4\sqrt{2}\varepsilon}{2(p-s)\eta + r'^2\varepsilon^2}, \quad \tan 2\theta_{13} \approx \sqrt{2}\sigma\eta, \quad \cos 2\theta_{23} \approx r'\varepsilon. \quad (50)$$

To obtain $\tan 2\theta_{12} = \mathcal{O}(1)$, we require that $|\eta| \gg \varepsilon^2$, suggesting $|\eta| \sim |\varepsilon|$. This texture exhibits

$$\cos 2\theta_{23} \approx \frac{\sigma(p-s)r'\tan 2\theta_{12}}{2} \sin \theta_{13}, \quad (51)$$

which suggests $\tan 2\theta_{12} \sim \sin \theta_{13} / \cos 2\theta_{23}$ similar to Eq.(24) for C2) of the normal mass hierarchy. There is also another correlation

$$\frac{\Delta m_{\odot}^2}{\Delta m_{atm}^2} \approx \frac{2\sqrt{2}}{r' \sin 2\theta_{12}} \cos 2\theta_{23}. \quad (52)$$

These two relations show

$$\frac{\Delta m_{\odot}^2}{\Delta m_{atm}^2} \approx \frac{\sqrt{2}\sigma(p-s)}{\cos 2\theta_{12}} \sin \theta_{13}. \quad (53)$$

The predictions $\Delta m_{\odot}^2 / \Delta m_{atm}^2$ and $\cos 2\theta_{23}$ are depicted in FIG.3-C2) and FIG.4-C2) as functions of $|\sin \theta_{13}|$. In these figures, $\sin \theta_{13}$ and $\cos 2\theta_{23}$ are constrained to satisfy

$$0.002 \lesssim |\sin \theta_{13}| (\lesssim 0.18), \quad 0.005 \lesssim |\cos 2\theta_{23}| \lesssim 0.05. \quad (54)$$

The result is expected because

- $\cos 2\theta_{23}$ determined by ε , whose magnitude is about $\sim 0.01 - 0.02$ from Eq.(49), yields $|\cos 2\theta_{23}| \sim 0.03 - 0.06$ for $r' = 3$,
- $\sin \theta_{13}$ determined by η , whose magnitude can be as large as 0.1 if $|p-s| \sim 0.1$ from Eq.(50) to balance $\varepsilon \sim 0.01 (\sim \Delta m_{\odot}^2 / \Delta m_{atm}^2)$, can have a broad range up to $\mathcal{O}(0.1)$.

This texture allows $|\eta| = \mathcal{O}(1)$, where the expressions of the masses and mixing angles based on $\eta^2 \ll 1$ are not appropriate. We have to use the correct ones listed in the Appendix A. The large $|\eta|$ region is marked by the grey dots in the figures.

C. Quasi Degenerate Mass Pattern I

1. Category C1) with $s_{23} \sim \sigma/\sqrt{2}$

This texture is only possible for C1). The mass ordering is given by $|m_1| \sim |m_2| \sim |m_3| \sim \mathcal{O}(\sqrt{\Delta m_{atm}^2})$. To describe $\Delta m_{\odot}^2 \ll \Delta m_{atm}^2$, the relation $m_1 \sim -m_2$ is imposed [26] instead of suppressing both m_1 and m_2 . In this texture, both mass patterns $|m_1| < |m_2| < |m_3|$ and $|m_3| < |m_1| < |m_2|$ are described consistently and are treated separately in our figures. The texture is specified by

$$M_{\nu}^{C1)} = d_0 \begin{pmatrix} -(2-\eta) & q+\varepsilon & -\sigma(q-\varepsilon) \\ q+\varepsilon & 1-r+r'\varepsilon & -\sigma(1+r) \\ -\sigma(q-\varepsilon) & -\sigma(1+r) & 1-r-r'\varepsilon \end{pmatrix}. \quad (55)$$

It should be noted that the texture with $r = 0$ coincides with the texture Eq.(34) for the inverted mass hierarchy. The corresponding texture for C2) is obtained by replacing σ by $-\sigma$ in $M_{\mu\tau}$ of Eq.(55). However, this replacement yields $\tan 2\theta_{13} = \mathcal{O}(1)$. Therefore, the texture for C2) with $m_1 \sim -m_2$ is not phenomenologically allowed.

The masses are calculated to be:

$$\begin{aligned} m_1 &\approx - \left(\frac{\sqrt{2}q}{\sin 2\theta_{12}} - \frac{\eta + 2(r-1)t_{13}^2 - 2((1+r)\Delta - \varepsilon r')\Delta}{2} \right) d_0, \\ m_2 &\approx \left(\frac{\sqrt{2}q}{\sin 2\theta_{12}} + \frac{\eta + 2(r-1)t_{13}^2 - 2((1+r)\Delta - \varepsilon r')\Delta}{2} \right) d_0, \\ m_3 &\approx [-2r + 2(1-r)t_{13}^2 + 2((1+r)\Delta - \varepsilon r')\Delta] d_0, \end{aligned} \quad (56)$$

and

$$\Delta m_{\odot}^2 \approx \frac{2\sqrt{2}q [\eta + 2(r-1)t_{13}^2 - 2((1+r)\Delta - \varepsilon r')\Delta]}{\sin 2\theta_{12}} d_0^2, \quad \Delta m_{atm}^2 \approx 4 \left| r^2 - \frac{2q^2}{\sin^2 2\theta_{12}} \right| d_0^2. \quad (57)$$

The mixing angles are given by

$$\tan 2\theta_{12} \approx \frac{q}{\sqrt{2}}, \quad \tan 2\theta_{13} \approx \frac{\sqrt{2}\sigma(2+2r-qr')}{q^2-2(r^2-1)}\varepsilon, \quad \cos 2\theta_{23} \approx 2\Delta, \quad (58)$$

where

$$\Delta = \frac{q+r'(1-r)}{q^2-2(r^2-1)}\varepsilon, \quad (59)$$

from which $q(\approx \sqrt{2}\tan 2\theta_{12}) \sim 3$ is expected.

There are two distinct realizations of $\Delta m_{\odot}^2/\Delta m_{atm}^2 \ll 1$. In the estimation of Δm_{\odot}^2 , if future experiments observe that $\sin^2 \theta_{13} \approx 0$, we obtain that

$$\Delta m_{\odot}^2 \approx \frac{4\eta}{\cos 2\theta_{12}} d_0^2, \quad \eta \sim \frac{\Delta m_{\odot}^2}{\Delta m_{atm}^2}, \quad (60)$$

leading to $\eta = \mathcal{O}(0.01)$, where we have used $q \approx \sqrt{2}\tan 2\theta_{12}$. However, if $\sin^2 \theta_{13} = \mathcal{O}(10^{-2})$, we find an interesting possibility that $\sin^2 \theta_{13}$ takes care of the mass hierarchy. Suppose that $\eta = 0$ in the texture, then, we reach

$$\Delta m_{\odot}^2 \approx \frac{4[2(r-1)s_{13}^2 - ((3+r)\Delta - 2\varepsilon r')\Delta]}{\cos 2\theta_{12}} d_0^2. \quad (61)$$

Because $\tan 2\theta_{13}$, and Δ are proportional to ε , Δm_{\odot} is proportional to $\sin^2 \theta_{13}$, leading to

$$\frac{\Delta m_{\odot}^2}{\Delta m_{atm}^2} \sim \sin^2 \theta_{13}. \quad (62)$$

There is also the proportionality of $\cos 2\theta_{23}$ to $\sin \theta_{13}$, which is given by

$$\cos 2\theta_{23} \approx \frac{2\sqrt{2}\sigma[q+r'(1-r)]}{2+2r-qr'} \sin \theta_{13}. \quad (63)$$

Since the neutrino masses are roughly controlled by $m_2 \sim m_1 \sim 2d_0/\cos 2\theta_{12}$ for $q \approx \sqrt{2}\tan 2\theta_{12}$ and $m_3 \sim -2rd_0$, we have the normal mass ordering: $|m_1| < |m_2| < |m_3|$ if $|r \cos 2\theta_{12}| > 1$, and the inverted mass ordering: $|m_3| < |m_1| < |m_2|$ if $|r \cos 2\theta_{12}| < 1$.

These features are reflected in the predictions $\Delta m_{\odot}^2/\Delta m_{atm}^2$ and $\cos 2\theta_{23}$ depicted in FIG.7 and FIG.8 for the normal mass ordering $|m_1| < |m_2| < |m_3|$ and in FIG.10 and FIG.11 for the inverted mass ordering $|m_3| < |m_1| < |m_2|$. We again use two regions: one with $|\eta| > 0.001$ and the other $|\eta| \leq 0.001$ to enhance the relationship of Eq.(62). In the normal mass ordering, there are two clusters around $\sin \theta_{13} \sim 0$ and $\sin \theta_{13} \sim 0.18$. In the first cluster for $\eta \neq 0$,

- the contribution from η in Δm_{\odot}^2 is enhanced because $\varepsilon \sim 0$ for $\sin \theta_{13} \sim 0$

while in the second cluster for $|\eta| \leq 0.001$,

- the contribution from ε^2 in Δm_{\odot}^2 is enhanced because $\eta \sim 0$.

Furthermore, if the texture is restricted to satisfy $r' < 0$, the second cluster consisting of the grey dots in FIG.7 becomes manifest itself. Because $1-r < 0$ for the normal mass ordering with $r \cos 2\theta_{12} > 1$, $r'(1-r) > 0$ for $r' < 0$ is satisfied in the numerator in Eq.(59) for $\cos 2\theta_{23}$. Therefore, this negative r' can enhance the size of $|\cos 2\theta_{23}|$. This region is shown by the triangle marks in FIG.8 with $|\eta| \leq 0.001$ and arises from the relation $\Delta m_{\odot}^2/\Delta m_{atm}^2 \sim \sin^2 \theta_{13}$, leading to the cluster around

$$0.14 \lesssim |\sin \theta_{13}| \lesssim 0.18, \quad 0.20 \lesssim |\cos 2\theta_{23}| \lesssim 0.25, \quad (64)$$

for the normal mass ordering. In the same figure for $r' > 0$, there are points giving 1) $|\cos 2\theta_{23}| \sim 0$ around $|\sin \theta_{13}| \sim 0.1$ and 2) $|\cos 2\theta_{23}| \sim 0.15$ around $|\sin \theta_{13}| \sim 0$. These points arise because

- for 1), $\cos 2\theta_{23}$ in Eq.(63) vanishes at $q \approx -r'(1-r)$ for $r > 1$, leading to $\tan 2\theta_{13} \approx \sqrt{2}\sigma\varepsilon/(1-r)$, which is about $\sin \theta_{13} \approx \sigma\varepsilon/[\sqrt{2}(1-r)]$ numerically found to be around 0.1, namely around $\mathcal{O}(\sqrt{\Delta m_\odot^2/\Delta m_{atm}^2})$,
- for 2), Δm_\odot^2 in Eq.(61) roughly requires that $|\Delta| \sim |\varepsilon| \sim 0.1$, namely, $|\cos 2\theta_{23}| \sim 0.1$, if $\sin \theta_{13} \sim 0$, which can be given by $2 + 2r - qr' \sim 0$ even if $\varepsilon \neq 0$ in Eq.(58).

On the other hand, in the inverted mass ordering, there is one cluster consisting of the grey dots in FIG.11 with $|\eta| \leq 0.001$, which gives the cluster around

$$0.05 \lesssim |\sin \theta_{13}| \lesssim 0.10, \quad 0.20 \lesssim \cos 2\theta_{23} \lesssim 0.32, \quad (65)$$

if r is restricted to satisfy $r < 0$. The reason to find this cluster is the same as that for the normal mass ordering. The positive $r'(1-r) > 0$ is obtained for $r < 0$ because r' is found to be positive in this region.

In our texture, the flavor mass of M_{ee} estimated to be $-(2-\eta)d_0$ corresponds to the effective neutrino mass $m_{\beta\beta}$ [32] used in the detection of the absolute neutrino mass [36]. Since $d_0 \sim \sqrt{\Delta m_{atm}^2}$, the size of $m_{\beta\beta}$ is roughly 0.1 eV. Two figures shown in FIG.9 and FIG.12 are the predictions of $m_{\beta\beta}$, respectively, for the normal mass ordering $|m_1| < |m_2| < |m_3|$, and the inverted mass ordering $|m_3| < |m_1| < |m_2|$. From these figures, $m_{\beta\beta}$ is estimated to give $m_{\beta\beta} \lesssim 0.05$ eV as expected, and at most $m_{\beta\beta} \sim 0.15$ eV for $|\eta| \leq 0.001$, which arises for $r \sim 1/\cos \theta_{12}$ that yields the larger d_0 from Eq.(57).

For the typical prediction with $\eta = 0$, let us choose $q = r = 3$, thus giving the normal mass ordering, and $r' = -1$, where $\sin^2 2\theta_{12} = 9/11$ is obtained, and we obtain that

$$\begin{aligned} \sin \theta_{13} &\approx -\frac{11\sigma\varepsilon}{7\sqrt{2}}, \quad \cos 2\theta_{23} = -\frac{10\varepsilon}{7}, \quad \Delta m_\odot^2 \approx 21d_0^2\varepsilon^2, \quad \Delta m_{atm}^2 = 14d_0^2, \\ m_2 \approx -m_1 &\approx \sqrt{\frac{11\Delta m_{atm}^2}{7}}, \quad m_3 \approx -\sqrt{\frac{18\Delta m_{atm}^2}{7}}, \quad m_{\beta\beta} \approx \sqrt{\frac{2\Delta m_{atm}^2}{7}}, \end{aligned} \quad (66)$$

leading to

$$\frac{\Delta m_\odot^2}{\Delta m_{atm}^2} \approx 1.2 \sin^2 \theta_{13}, \quad (67)$$

which gives $0.15 \lesssim |\sin \theta_{13}| \lesssim 0.18$ giving $0.12 \lesssim |\cos 2\theta_{23}| \lesssim 0.15$ to recover the observed values of $\Delta m_\odot^2/\Delta m_{atm}^2$, which is consistent with the region of the cluster near $|\sin \theta_{13}| \sim 0.18$.

D. Quasi Degenerate Mass Pattern II

The mass ordering is given by $|m_1| \sim |m_2| \sim |m_3|$ with the hierarchy of $|m_i^2 - m_j^2| \ll m_{1,2,3}^2$ ($i, j = 1, 2, 3$). For our numerical calculation, we use $|m_{1,2,3}| \geq \sqrt{\Delta m_{atm}^2}$ and we further require $4|\eta| \leq 1/3$ to favor $|m_i^2 - m_j^2| \ll m_{1,2,3}^2$ ($i, j = 1, 2, 3$) because $m_{1,2,3}^2 \sim \Delta m_{atm}^2/4|\eta|$ is to be obtained. Since there should be three distinct mass scales, textures will involve terms proportional to η^2 , and $\eta\varepsilon$ in addition to the ordinary terms proportional to η , and ε to produce the hierarchy. Textures are characterized by the relative sign of m_3 as $m_1 \sim m_2 \sim m_3$ or $m_1 \sim m_2 \sim -m_3$. In textures with $m_1 \sim m_2 \sim -m_3$, the flavor neutrino masses should satisfy that $|d - \sigma e - a| \lesssim \mathcal{O}(\eta^2)$ as well as $b + \varepsilon\Delta b' = \mathcal{O}(\eta^2, \varepsilon^2)$ for C1) and $|d + \sigma e - a| \lesssim \mathcal{O}(\eta^2)$ as well as $\varepsilon b' + \Delta b = \mathcal{O}(\eta\varepsilon)$ for C2). The basic structure for each mass matrix is given by

$$\begin{pmatrix} 1 & 0 & 0 \\ 0 & 1 & 0 \\ 0 & 0 & 1 \end{pmatrix}, \quad \begin{pmatrix} 1 & 0 & 0 \\ 0 & 0 & 1 \\ 0 & 1 & 0 \end{pmatrix}, \quad (68)$$

for the textures with $m_1 \sim m_2 \sim m_3$ and with $m_1 \sim m_2 \sim -m_3$, respectively. The latter texture has an approximate $L_\mu - L_\tau$ conservation, whose influence on neutrino oscillations has been lately discussed in Ref.[34, 35].

$$1. \quad m_1 \sim m_2 \sim m_3$$

$$1-1. \text{ Category C1) with } s_{23} \sim \sigma/\sqrt{2}$$

The texture is given by

$$M_\nu^{C1)} = d_0 \begin{pmatrix} 1 - \eta & (q\eta + \varepsilon)\eta & -\sigma(q\eta - \varepsilon)\eta \\ (q\eta + \varepsilon)\eta & 1 + r'\varepsilon\eta & \sigma(1 - s\eta)\eta \\ -\sigma(q\eta - \varepsilon)\eta & \sigma(1 - s\eta)\eta & 1 - r'\varepsilon\eta \end{pmatrix}. \quad (69)$$

Neutrino masses are predicted to be:

$$m_1 \approx \left(1 - \eta - \frac{\sqrt{2}(2q\eta - r'\varepsilon^2)\eta}{2\sin 2\theta_{12}}\right) d_0, \quad m_2 \approx \left(1 - \eta + \frac{\sqrt{2}(2q\eta - r'\varepsilon^2)\eta}{2\sin 2\theta_{12}}\right) d_0, \\ m_3 \approx (1 + \eta) d_0, \quad (70)$$

and

$$\Delta m_\odot^2 \approx \frac{2\sqrt{2}(2q\eta - r'\varepsilon^2)\eta d_0^2}{\sin 2\theta_{12}}, \quad \Delta m_{atm}^2 \approx 4|\eta|d_0^2, \quad (71)$$

and mixing angles are

$$\tan 2\theta_{12} \approx \frac{2\sqrt{2}(2q\eta - r'\varepsilon^2)}{2s\eta + (2 - r'^2)\varepsilon^2}, \quad \tan 2\theta_{13} \approx \sqrt{2}\sigma\varepsilon, \quad \cos 2\theta_{23} \approx -r'\varepsilon. \quad (72)$$

The parameter ε relates $\cos 2\theta_{23}$ to $\sin \theta_{13}$:

$$\cos 2\theta_{23} \approx -\sqrt{2}\sigma r' \sin \theta_{13}, \quad (73)$$

which indicates $|\cos 2\theta_{23}| \sim |\sin \theta_{13}|$. It should be noted that the predictions of $\Delta m_{atm}^2/\Delta m_\odot^2$ and $\cos 2\theta_{23}$ are very similar to those for the inverted mass hierarchy in C1). Therefore, the figures FIG.13-C1) and FIG.14 -C1) for $m_1 \sim m_2 \sim m_3$ are almost identical to FIG.3-C1) and FIG.4 -C1).

The largest size of the mass scales is d_0 , which is approximately $m_{\beta\beta}(= M_{ee})$. Then, we find the following mass ordering:

$$m_{\beta\beta}^2 : \Delta m_{atm}^2 : \Delta m_\odot^2 \sim 1 : |\eta| : \left(\eta - \frac{r'\varepsilon^2}{2}\right)\eta. \quad (74)$$

Shown in FIG.15-C1) for $m_1 \sim m_2 \sim m_3$ is the estimation of $m_{\beta\beta}$ as a function of $|\sin \theta_{13}|$. We observe that $m_{\beta\beta}$ can take larger values as $|\sin \theta_{13}|$ gets larger. This is because

- $|\eta|$ can be as small as possible if $|\sin \theta_{13}| = \mathcal{O}(0.01)$,

where the size of $\Delta m_\odot^2/\Delta m_{atm}^2$ is taken care of by $\sin \theta_{13}$ via ε^2 . It is in fact this value of $|\sin \theta_{13}| = \mathcal{O}(0.01)$ that $m_{\beta\beta}$ begins to increase. The figure shows that $m_{\beta\beta}$ is in the range of

$$0.1 \text{ eV} \lesssim m_{\beta\beta} \lesssim 0.5 \text{ eV}. \quad (75)$$

This predicted values of $m_{\beta\beta}$ are inside $0.22 \text{ eV} \lesssim m_{\beta\beta} \lesssim 1.6 \text{ eV}$ obtained from the Heidelberg-Moscow experiment [37]. Our prediction is within reach of future planned experiments measuring $m_{\beta\beta}$ [38].

1-2. Category C2) with $s_{23} \sim -\sigma/\sqrt{2}$

The quasi degenerate mass pattern in this case has the mass matrix with $M_{\mu\tau} \rightarrow -M_{\mu\tau}$ in $M_\nu^{C1)}$, and is given by

$$M_\nu^{C2)} = d_0 \begin{pmatrix} 1 - \eta & (q\eta + \varepsilon)\eta & -\sigma(q\eta - \varepsilon)\eta \\ (q\eta + \varepsilon)\eta & 1 + r'\varepsilon\eta & -\sigma(1 - s\eta)\eta \\ -\sigma(q\eta - \varepsilon)\eta & -\sigma(1 - s\eta)\eta & 1 - r'\varepsilon\eta \end{pmatrix}. \quad (76)$$

Neutrino masses are predicted to be:

$$m_1 \approx \left(1 - \eta - \frac{\sqrt{2}\varepsilon\eta}{\sin 2\theta_{12}}\right) d_0, \quad m_2 \approx \left(1 - \eta + \frac{\sqrt{2}\varepsilon\eta}{\sin 2\theta_{12}}\right) d_0, \quad m_3 \approx (1 + \eta) d_0, \quad (77)$$

and

$$\Delta m_{\odot}^2 \approx \frac{4\sqrt{2}\varepsilon\eta d_0^2}{\sin 2\theta_{12}}, \quad \Delta m_{atm}^2 \approx 4|\eta|d_0^2, \quad (78)$$

and mixing angles are

$$\tan 2\theta_{12} \approx \frac{4\sqrt{2}\varepsilon}{s\eta - r'^2\varepsilon^2}, \quad \tan 2\theta_{13} \approx -\sqrt{2}\sigma q\eta, \quad \cos 2\theta_{23} \approx -r'\varepsilon. \quad (79)$$

The prediction of $\tan 2\theta_{12}$ indicates that $|\eta| \sim |\varepsilon|$ to have $\tan 2\theta_{12} = \mathcal{O}(1)$. The requirement of $|\eta| \sim |\varepsilon|$ gives

$$\cos 2\theta_{23} \approx \frac{\sigma r' s \tan 2\theta_{12}}{4q} \sin \theta_{13}, \quad (80)$$

leading to $\tan 2\theta_{12} \sim \cos 2\theta_{23} / \sin \theta_{13}$. The mass hierarchy is characterized by ε instead of η in C1), and can be cast into the form of

$$\frac{\Delta m_{\odot}^2}{\Delta m_{atm}^2} \approx -\frac{\sqrt{2}\kappa \cos 2\theta_{23}}{r' \sin 2\theta_{12}}, \quad (81)$$

where $\kappa = \eta/|\eta|$, from which we find that $0.006 \lesssim |\cos 2\theta_{23}| \lesssim 0.1$ from $\sqrt{2}|\cos 2\theta_{23}/r'| \lesssim 0.045$ for $1/3 \leq |r'| \leq 3$ to yield $\Delta m_{\odot}^2/\Delta m_{atm}^2 \approx \sqrt{2}|\cos 2\theta_{23}/r'| = 0.025 - 0.048$. From Eqs.(80) and (81), we observe that

$$\frac{\Delta m_{\odot}^2}{\Delta m_{atm}^2} \approx -\frac{\sqrt{2}\sigma\kappa s}{4q \cos 2\theta_{12}} \sin \theta_{13}. \quad (82)$$

The effective neutrino mass $m_{\beta\beta}$ is given by $(1 - \eta)d_0$. There is a possibility of having an enhanced $m_{\beta\beta}$ for $\eta \sim 0$, which satisfies

$$m_{\beta\beta}^2 : \Delta m_{atm}^2 : \Delta m_{\odot}^2 \sim 1 : |\eta| : |\eta\varepsilon|. \quad (83)$$

The predictions of $\Delta m_{\odot}^2/\Delta m_{atm}^2$, and $\cos 2\theta_{23}$ are plotted in FIG.13-C2) and FIG.14-C2), both for $m_1 \sim m_2 \sim m_3$, where η is restricted to satisfy $4|\eta| \leq 1/3$ to give $|m_1^2| \sim \Delta m_{atm}^2/4|\eta| \geq 3\Delta m_{atm}^2$. In all figures, plots are marked by the black dots satisfying $4|\eta| \leq 1/3$ and, for comparison, by the grey dots satisfying $4|\eta| > 1/3$. In FIG.14-C2) for $m_1 \sim m_2 \sim m_3$, $\cos 2\theta_{23}$ does not vanish and bounded as $|\cos 2\theta_{23}| \lesssim 0.1$. This result is consistent with our expectation based on

- $\Delta m_{\odot}^2/\Delta m_{atm}^2 \approx \sqrt{2}|\cos 2\theta_{23}/r'|$ giving $0.006 \lesssim |\cos 2\theta_{23}| \lesssim 0.1$.

From this figure, we find that

$$0.005 \lesssim |\cos 2\theta_{13}| \lesssim 0.1, \quad (84)$$

while $|\sin \theta_{13}|$ covers all the allowed values owing to the parameter q in Eq.(79).

Let us estimate $m_{\beta\beta}$ for $\sin^2 2\theta_{12} = 0.8$. The choice of $\varepsilon = 0.02$ leads to $\Delta m_{\odot}^2/\Delta m_{atm}^2 = 3.2 \times 10^{-2}$, which gives $|\eta|d_0^2 = 6.4 \times 10^{-4}$ for $\Delta m_{\odot}^2 = 8 \times 10^{-5} \text{ eV}^2$, corresponding to $\Delta m_{atm}^2 = 2.56 \times 10^{-3} \text{ eV}^2$. This estimation gives $m_{\beta\beta} = 2.5 \times 10^{-2}/\sqrt{|\eta|} \text{ eV}$, leading to $m_{\beta\beta} = 0.18\sqrt{|\varepsilon/\eta|} \text{ eV}$. In FIG.15-C2) for $m_1 \sim m_2 \sim m_3$, the larger $m_{\beta\beta}$ is realized by the smaller $|\sin \theta_{13}|$. This feature is a result of

- Eq.(83) supplemented by $|\eta| \sim |\varepsilon|$ giving $|\eta| \sim |\sin \theta_{13}|$,

which indicates that $\sin \theta_{13} \rightarrow 0$ as $\eta \rightarrow 0$. The figure shows

$$0.07 \text{ eV} \lesssim m_{\beta\beta} \lesssim 0.35 \text{ eV}, \quad (85)$$

for the black dots.

$$2. \quad m_1 \sim m_2 \sim -m_3$$

2-1. Category C1) with $s_{23} \sim \sigma/\sqrt{2}$

The texture is given by

$$M_\nu^{C1)} = d_0 \begin{pmatrix} 1 + \eta & q\eta^2 + \varepsilon & -\sigma(q\eta^2 - \varepsilon) \\ q\eta^2 + \varepsilon & \eta + r'\varepsilon & -\sigma \\ -\sigma(q\eta^2 - \varepsilon) & -\sigma & \eta - r'\varepsilon \end{pmatrix}, \quad (86)$$

which satisfies that $d - \sigma e - a = 0$ and $b + \varepsilon \Delta b' = \mathcal{O}(\eta^2, \varepsilon^2)$ to yield $\tan 2\theta_{12} = \mathcal{O}(1)$. Neutrino masses are predicted to be:

$$\begin{aligned} m_1 &\approx \left(1 + \eta + \frac{(2 + r'^2) \varepsilon^2}{4} - \frac{2q\eta^2 + r'\varepsilon^2}{\sqrt{2} \sin 2\theta_{12}} \right) d_0, \\ m_3 &\approx \left(1 + \eta + \frac{(2 + r'^2) \varepsilon^2}{4} + \frac{2q\eta^2 + r'\varepsilon^2}{\sqrt{2} \sin 2\theta_{12}} \right) d_0, \\ m_2 &\approx - \left(1 - \eta + \frac{(2 + r'^2) \varepsilon^2}{2} \right) d_0, \end{aligned} \quad (87)$$

and

$$\Delta m_\odot^2 \approx \frac{2\sqrt{2} (2q\eta^2 + r'\varepsilon^2) d_0^2}{\sin 2\theta_{12}}, \quad \Delta m_{atm}^2 \approx \left| 4\eta - \frac{(2 + r'^2) \varepsilon^2}{2} \right| d_0^2, \quad (88)$$

and mixing angles are

$$\tan 2\theta_{12} \approx \frac{2\sqrt{2} (2q\eta^2 + r'\varepsilon^2)}{(2 + r'^2) \varepsilon^2}, \quad \tan 2\theta_{13} \approx -\sqrt{2}\sigma\varepsilon, \quad \cos 2\theta_{23} \approx r'\varepsilon. \quad (89)$$

The parameter ε is common in $\cos 2\theta_{23}$ and $\sin \theta_{13}$ and yields

$$\cos 2\theta_{23} \approx -\sqrt{2}\sigma r' \sin \theta_{13}. \quad (90)$$

There is a constraint on η to yield $\tan 2\theta_{12} = \mathcal{O}(1)$, which requires that $|\eta| \lesssim |\varepsilon|$. Another constraint arises from the requirement of $\Delta m_\odot^2 / \Delta m_{atm}^2 = \mathcal{O}(0.01)$. If $|\eta| \lesssim \varepsilon^2$, we obtain $\Delta m_{atm}^2 \sim \varepsilon^2 d_0^2$, giving $\Delta m_\odot^2 / \Delta m_{atm}^2 \gtrsim 1$. Therefore, we need to have $|\eta| \gg \varepsilon^2$, suggesting that $|\eta| \gtrsim |\varepsilon|$. The two constraints of $|\eta| \lesssim |\varepsilon|$ and $|\eta| \gtrsim |\varepsilon|$ are satisfied if $|\eta| \sim |\varepsilon|$. The mass hierarchy is given by

$$\frac{\Delta m_\odot^2}{\Delta m_{atm}^2} \approx \frac{1}{\sqrt{2} \sin 2\theta_{12}} \left(2q|\eta| + r' \frac{\varepsilon^2}{|\eta|} \right), \quad (91)$$

from which we find that

1. $|\eta|$ is constrained to be $\mathcal{O}(0.01)$ by $\Delta m_\odot^2 / \Delta m_{atm}^2$ if $qr' > 0$,
2. $|\eta|$ is not constrained by $\Delta m_\odot^2 / \Delta m_{atm}^2$ but the size of $2|\eta| - (|r'\varepsilon^2|/|q\eta|)$ is constrained if $qr' < 0$.

Larger values of $|\eta|$ ($\gtrsim 0.01$) are only possible for the texture with $qr' < 0$. This range of $|\eta|$ affects the size of the mass scale d_0 , which is approximately $m_{\beta\beta}$. The following mass ordering is found in this texture:

$$m_{\beta\beta}^2 : \Delta m_{atm}^2 : \Delta m_\odot^2 \sim 1 : |\eta| : \eta^2 + \frac{r'}{2q} \varepsilon^2. \quad (92)$$

The larger $m_{\beta\beta}$ is obtained for the smaller $|\eta|$. Since $|\eta|$ can be as small as 0.01, we expect that $m_{\beta\beta} \sim \sqrt{\Delta m_{atm}^2 / |\eta|} \sim 0.5$ eV.

The predictions $\Delta m_\odot^2 / \Delta m_{atm}^2$ and $\cos 2\theta_{23}$ are depicted in FIG.13-C1) and FIG.14 -C1) for $m_1 \sim m_2 \sim -m_3$. In FIG.14-C1) for $m_1 \sim m_2 \sim -m_3$, there are almost straight lines originating from $\sin \theta_{13} \sim 0$. This appearance of these lines is due to

- the proportionality of $\cos 2\theta_{23}$ to $\sin \theta_{13}$ of Eq.(90).

From these figures for the black dots, we find that

$$|\cos 2\theta_{23}| \lesssim 0.15, \quad |\sin \theta_{13}| \lesssim 0.06. \quad (93)$$

Shown in FIG.15-C1) for $m_1 \sim m_2 \sim -m_3$ is the size of $m_{\beta\beta}$, which is in the range of

$$0.07 \text{ eV} \lesssim m_{\beta\beta} \lesssim 0.50 \text{ eV}. \quad (94)$$

The figure shows that larger values of $m_{\beta\beta}$ are produced by smaller values of $|\sin \theta_{13}|$. This behavior can be understood because we know that

- $m_{\beta\beta}$ gets larger as $|\eta|$ gets smaller from Eq.(92),

where the smallness of $|\eta|$ is converted into that of $|\sin \theta_{13}|$ from $|\eta| \sim |\epsilon|$.

2-2. Category C2) with $s_{23} \sim -\sigma/\sqrt{2}$

The quasi degenerate mass pattern is given by:

$$M_\nu^{C2)} = d_0 \begin{pmatrix} 1 + \eta & (q + \varepsilon)\eta & -\sigma(q - \varepsilon)\eta \\ (q + \varepsilon)\eta & \eta + r'\varepsilon & \sigma \\ -\sigma(q - \varepsilon)\eta & \sigma & \eta - r'\varepsilon \end{pmatrix}, \quad (95)$$

which satisfies that $d + \sigma e - a = 0$ and $\varepsilon b' + \Delta b = \mathcal{O}(\eta\varepsilon)$ to yield $\tan 2\theta_{12} = \mathcal{O}(1)$. Neutrino masses are predicted to be:

$$\begin{aligned} m_1 &\approx \left(1 + \eta - \frac{3r'^2\varepsilon^2}{4} - \frac{\sqrt{2}(2 - qr')\varepsilon\eta}{2\sin 2\theta_{12}}\right) d_0, \\ m_2 &\approx \left(1 + \eta - \frac{3r'^2\varepsilon^2}{4} + \frac{\sqrt{2}(2 - qr')\varepsilon\eta}{2\sin 2\theta_{12}}\right) d_0, \\ m_3 &\approx -\left(1 - \eta - \frac{3r'^2\varepsilon^2}{4}\right) d_0, \end{aligned} \quad (96)$$

and

$$\Delta m_\odot^2 \approx \frac{2\sqrt{2}(2 - qr')\varepsilon\eta d_0^2}{\sin 2\theta_{12}}, \quad \Delta m_{atm}^2 \approx \left|4\eta + \frac{3r'^2\varepsilon^2}{2}\right| d_0^2, \quad (97)$$

and mixing angles are

$$\tan 2\theta_{12} \approx \frac{2\sqrt{2}(qr' - 2)\varepsilon\eta}{2q^2\eta^2 + 3r'^2\varepsilon^2}, \quad \tan 2\theta_{13} \approx \sqrt{2}\sigma q\eta, \quad \cos 2\theta_{23} \approx -\varepsilon r'. \quad (98)$$

To obtain $\tan 2\theta_{12} = \mathcal{O}(1)$ is possible if $|\eta| \sim |\varepsilon|$, which is translated into $|\cos 2\theta_{23}| \propto |\sin \theta_{13}|$. The mass hierarchy is given by

$$\frac{\Delta m_\odot^2}{\Delta m_{atm}^2} \approx \frac{\kappa(qr' - 2)\cos 2\theta_{23}}{\sqrt{2}r'\sin 2\theta_{12}}, \quad (99)$$

where κ stands for the sign of η . The effective neutrino mass $m_{\beta\beta}$ given by $(1 + \eta)d_0$ satisfies the same ordering as Eq.(83) for $m_1 \sim m_2 \sim m_3$ described by

$$m_{\beta\beta}^2 : \Delta m_{atm}^2 : \Delta m_\odot^2 \sim 1 : |\eta| : |\eta\varepsilon|. \quad (100)$$

This relation shows that large sizes of $m_{\beta\beta}$ favor small values of $|\eta|$.

The predictions of $\Delta m_\odot^2/\Delta m_{atm}^2$, and $\cos 2\theta_{23}$ are plotted in FIG.13-C2) and FIG.14-C2), both for $m_1 \sim m_2 \sim -m_3$, as functions of $|\sin \theta_{13}|$. The gross features are similar to those for C1). We find that

$$0.005 \lesssim |\cos 2\theta_{23}| \lesssim 0.30, \quad |\sin \theta_{13}| \lesssim 0.14, \quad (101)$$

for $4|\eta| \leq 1/3$. The effective neutrino mass $m_{\beta\beta}$ is plotted in FIG.15-C2) for $m_1 \sim m_2 \sim -m_3$, where $m_{\beta\beta}$ gets larger as $|\sin \theta_{13}|$ gets smaller as indicated by $m_{\beta\beta} \sim \sqrt{\Delta m_{atm}^2/|\sin \theta_{13}|}$. We observe that

$$m_{\beta\beta} \gtrsim 0.07 \text{ eV}, \quad (102)$$

which becomes as large as 0.5 eV for $\sin \theta_{13} \sim 0$.

IV. SUMMARY AND DISCUSSIONS

We have clarified the effects from the μ - τ symmetry breaking in neutrino mass textures. Possible forms of the textures are summarized in TABLE I, where the relations among $\cos 2\theta_{23}$, $\sin \theta_{13}$, and $\Delta m_{\odot}^2/\Delta m_{atm}^2$ are listed. These relations reflect the general property discussed in Ref. [22]. We have found the relations:

$$|\cos 2\theta_{23}| \sim \sin \theta_{23}, \quad |\cos 2\theta_{23}| \sin \theta_{13} \sim \frac{\Delta m_{\odot}^2}{\Delta m_{atm}^2}, \quad |\cos 2\theta_{23}| \sim \frac{\Delta m_{\odot}^2}{\Delta m_{atm}^2}, \quad (103)$$

depending on the type of textures, where the possible signs are ignored. Two qualitatively different textures are classified as C1), and C2), respectively, according to the behavior of $\sin \theta_{13} \rightarrow 0$, and $\sin \theta_{12} \rightarrow 0$ in the μ - τ symmetric limit. It would be curious to have $\sin \theta_{12} = 0$ in the symmetric limit because the textures indeed give $\sin^2 2\theta_{12} = \mathcal{O}(1)$, which does not seem to vanish. The reason is that, in the textures for C2), $\tan 2\theta_{12}$ is expressed as

$$\tan 2\theta_{12} \approx \frac{4\sqrt{2}\varepsilon}{2(s-p)\eta - r'^2\varepsilon^2}, \quad (104)$$

$$\tan 2\theta_{12} \approx \frac{4\sqrt{2}\varepsilon}{2p\eta + r'^2\varepsilon^2}, \quad (105)$$

$$\tan 2\theta_{12} \approx \frac{4\sqrt{2}\varepsilon}{2s\eta - r'^2\varepsilon^2}, \quad (106)$$

$$\tan 2\theta_{12} \approx \frac{2\sqrt{2}(qr' - 2)\varepsilon\eta}{2q^2\eta^2 + 3r'^2\varepsilon^2}, \quad (107)$$

respectively, for the normal mass hierarchy, the inverted mass hierarchy, the quasi degenerate mass pattern II with $m_1 \sim m_2 \sim m_3$, and the quasi degenerate mass pattern II with $m_1 \sim m_2 \sim -m_3$. It is thus obvious that $\tan 2\theta_{12} \rightarrow 0$ as $\varepsilon \rightarrow 0$, restoring the μ - τ symmetry. From Eqs.(104) -(106), we have observed that $\tan 2\theta_{12}$ is roughly estimated to be

$$\tan 2\theta_{12} \sim \frac{\cos 2\theta_{23}}{\sin \theta_{13}}, \quad (108)$$

which is specific to C2).

The differences in the same mass hierarchy can be found in Eq.(103) as in TABLE.I, where precise determination of $\sin \theta_{13}$, $\sin^2 2\theta_{23}$, and $\Delta m_{\odot}^2/\Delta m_{atm}^2$ may select one of the relations. The differences in the prediction of $\cos 2\theta_{23}$ can also be read off from the figures, where each texture shows its specific pattern. From the scattered plots, we may exclude some of textures with certain ranges of mixing angles. When future experiments observe

1. $|\sin \theta_{13}| = 0.16 - 0.18$ as large as the present upper bound, textures giving

- the normal mass hierarchy
 - in C1) if $|\cos 2\theta_{23}| \lesssim 0.05$,
 - in C2) if $|\cos 2\theta_{23}| \lesssim 0.03$,
- the inverted mass hierarchy
 - in C1) with $m_1 \sim m_2$ if $|\cos 2\theta_{23}| \lesssim 0.10$,
 - in C1) with $m_1 \sim -m_2$ for $\eta \neq 0$ if $|\cos 2\theta_{23}| \gtrsim 0.10$ and for $\eta \neq 0$,
 - in C2) with $m_1 \sim m_2$ if $|\cos 2\theta_{23}| \gtrsim 0.07$,
- the quasi degenerate mass pattern I exclusively in C1)
 - with the normal mass ordering if $|\cos 2\theta_{23}| \lesssim 0.05$,
 - with the inverted mass ordering if $|\cos 2\theta_{23}| \lesssim 0.10$,
- the quasi degenerate mass pattern II
 - in C1) with $m_1 \sim m_2 \sim m_3$ if $|\cos 2\theta_{23}| \lesssim 0.07$,
 - in C2) with $m_1 \sim m_2 \sim m_3$ if $|\cos 2\theta_{23}| \gtrsim 0.10$,
 - in C1) and C2) with $m_1 \sim m_2 \sim -m_3$,

are excluded;

2. $|\sin \theta_{13}| \lesssim 0.02$ as an almost vanishing $|\sin \theta_{13}|$, textures giving

- the normal mass hierarchy
 - in C1) if $|\cos 2\theta_{23}| \gtrsim 0.13$.
 - in C2) if $|\cos 2\theta_{23}| \gtrsim 0.05$,
- the inverted mass hierarchy
 - in C1) with $m_1 \sim m_2$ if $|\cos 2\theta_{23}| \gtrsim 0.10$,
 - in C2) with $m_1 \sim -m_2$ for $|\eta| \leq 0.001$,
- the quasi degenerate mass pattern I exclusively in C1)
 - with the normal mass ordering for $|\eta| \leq 0.01$ if $|\cos 2\theta_{23}| \lesssim 0.05$ and $|\cos 2\theta_{23}| \gtrsim 0.20$,
 - with the inverted mass ordering for $|\eta| \leq 0.01$ if $|\cos 2\theta_{23}| \lesssim 0.07$,
- the quasi degenerate mass pattern II
 - in C1) and C2) with $m_1 \sim m_2 \sim \pm m_3$ if $|\cos 2\theta_{23}| \gtrsim 0.10$,

are excluded.

Similarly, if $m_{\beta\beta}$ is observed to be ~ 0.35 eV, textures giving the quasi degenerate mass pattern II

- in C1) with $m_1 \sim m_2 \sim m_3$ if $|\sin \theta_{13}| \lesssim 0.04$,
- in C2) with $m_1 \sim m_2 \sim m_3$ and in C1) and C2) with $m_1 \sim m_2 \sim -m_3$ if $|\sin \theta_{13}| \gtrsim 0.02$,

are excluded.

Most of textures contain two small parameters ε , and η . The smallness of ε is obviously ascribed to the tiny μ - τ symmetry breaking. However, the reason to have the small η is not clear. There is a possibility that textures for the normal mass hierarchy may be protected by the electron number conservation, whose tiny violation can take care of the smallness of η [20, 21]. As stated in Eq.(19), the flavor neutrino masses naturally satisfy that $M_{ee} : M_{ei} : M_{ij} \sim \eta^2 : \eta : 1$ for $i, j = \mu, \tau$. We have also shown that the smallness of ε is always linked to that of $\cos 2\theta_{23}$. Another interesting possibility arises from the texture where the tiny quantities are just supplied by the μ - τ symmetry breaking parameter ε . It is described by the specific form

$$M_\nu = d_0 \begin{pmatrix} -2 & q + \varepsilon & -\sigma(q - \varepsilon) \\ q + \varepsilon & 1 - r + r'\varepsilon & -\sigma(1 + r) \\ -\sigma(q - \varepsilon) & -\sigma(1 + r) & 1 - r - r'\varepsilon \end{pmatrix}, \quad (109)$$

for the quasi degenerate mass pattern I with $r \neq 0$. If $r = 0$, this texture gives the inverted mass hierarchy. These two textures are solely available for C1) with $m_1 \sim -m_2$, and does not contain the additional small parameter η . Furthermore, we have demonstrated that these two textures can provide

$$\frac{\Delta m_\odot^2}{\Delta m_{atm}^2} \sim \sin^2 \theta_{13}, \quad (110)$$

where $\sin^2 \theta_{13}$ is, respectively, estimated to be:

$$0.02 \lesssim |\sin \theta_{13}| \lesssim 0.10, \quad 0.14 \lesssim |\sin \theta_{13}| \lesssim 0.18, \quad \text{and} \quad 0.04 \lesssim |\sin \theta_{13}| \lesssim 0.10, \quad (111)$$

for the inverted mass hierarchy, the quasi degenerate mass pattern I with the normal mass ordering, and the quasi degenerate mass pattern I with the inverted mass ordering. It should be noted here that we have to retain all the terms of $\mathcal{O}(\sin^2 \theta_{13})$, which consist of any second order combinations of $\sin \theta_{13} (\approx \varepsilon)$, and $\cos 2\theta_{23} (\approx 2\Delta)$.

The similar predictions are obtained in the textures for C2) which predict $\Delta m_\odot^2 \propto \eta\varepsilon$ (or $\Delta m_\odot^2 \propto \varepsilon$), $\sin \theta_{13} \propto \eta$ and $\tan 2\theta_{12} \propto \varepsilon/\eta$. From the collaboration between η and ε , we have found that

$$\frac{\Delta m_\odot^2}{\Delta m_{atm}^2} (\propto \eta\varepsilon) \sim \tan 2\theta_{12} \sin^2 \theta_{13}, \quad |\sin \theta_{13}| \gtrsim 0.06, \quad (112)$$

for the normal mass hierarchy, and

$$\frac{\Delta m_\odot^2}{\Delta m_{atm}^2} (\propto \varepsilon) \sim \tan 2\theta_{12} \sin \theta_{13}, \quad 0.002 \lesssim |\sin \theta_{13}| \lesssim 0.03, \quad (113)$$

for the inverted mass hierarchy. These are the relations discussed in Ref.[24, 25].

We expect the following scenarios based on the symmetry argument to emerge: Underlying dynamics creating neutrino masses may possess

- the approximate μ - τ symmetry to induce the textures Eq.(34) and Eq.(55) in the case of C1), respectively, for the quasi degenerate mass pattern I, and the inverted mass hierarchy, or
- the approximate μ - τ symmetry as well as the approximate electron number conservation to induce the texture Eq.(13) in the case of C1), or Eq.(20) in the case of C2), both for the normal mass hierarchy.

To see the corresponding lagrangians, $\mathcal{L}_{\text{inverted}}^{C1)}$ for Eq.(34), $\mathcal{L}_{\text{normal}}^{C1)}$ for Eq.(55), $\mathcal{L}_{\text{normal}}^{C1-e)}$ for Eq.(13), and $\mathcal{L}_{\text{normal}}^{C2-e)}$ for Eq.(20), it is convenient to use $\nu_{\pm} = (\nu_{\mu} \pm (-\sigma)\nu_{\tau})/\sqrt{2}$, where $\nu_{+(-)}$ is an even (odd) state with respect to the μ - τ exchange. In terms of ν_{\pm} the lagrangians are described by

$$\begin{aligned}
-\mathcal{L}_{\text{inverted}}^{C1)} &= \frac{d_0}{2} \left[2(\nu_{+}\nu_{+} - \nu_e\nu_e) + \sqrt{2}q(\nu_e\nu_{+} + \nu_{+}\nu_e) \right] + \mathcal{L}_b, \\
-\mathcal{L}_{\text{normal}}^{C1)} &= \frac{d_0}{2} \left[2(\nu_{+}\nu_{+} - r\nu_{-}\nu_{-} - \nu_e\nu_e) + \sqrt{2}q(\nu_e\nu_{+} + \nu_{+}\nu_e) \right] + \mathcal{L}_b, \\
-\mathcal{L}_{\text{normal}}^{C1-e)} &= \frac{d_0}{2} \left[2\nu_{-}\nu_{-} + \eta \left(s(\nu_{+}\nu_{+} - \nu_{-}\nu_{-}) + \sqrt{2}(\nu_e\nu_{+} + \nu_{+}\nu_e) \right) + p'\eta^2\nu_e\nu_e \right] + \mathcal{L}_b, \\
-\mathcal{L}_{\text{normal}}^{C2-e)} &= \frac{d_0}{2} \left[2\nu_{+}\nu_{+} + \eta \left(s(\nu_{-}\nu_{-} - \nu_{+}\nu_{+}) + \sqrt{2}(\nu_e\nu_{+} + \nu_{+}\nu_e) \right) + p'\eta^2\nu_e\nu_e \right] + \mathcal{L}_b,
\end{aligned} \tag{114}$$

for p' from $p = p'\eta$, where \mathcal{L}_b is given by

$$\mathcal{L}_b = \frac{\varepsilon d_0}{2} \left[\sqrt{2}(\nu_e\nu_{-} + \nu_{-}\nu_e) + r'(\nu_{+}\nu_{-} + \nu_{-}\nu_{+}) \right], \tag{115}$$

as the μ - τ symmetry breaking lagrangian. In $\mathcal{L}_{\text{normal,inverted}}^{C1)}$, the relative strength of $\nu_e\nu_e$ over $\nu_{+}\nu_{+}$ should be exactly -1 . Similarly, in $\mathcal{L}_{\text{inverted}}^{C1)}$ and $\mathcal{L}_{\text{normal}}^{C2-e)}$ (or $\mathcal{L}_{\text{normal}}^{C1-e)}$, the μ - τ symmetric term of $\nu_{+}\nu_{+}$ (or $\nu_{-}\nu_{-}$) that remains at $\eta = 0$ is absent. The appearance of such specific forms of the textures may call for additional underlying symmetries. For instance, the absence of $\nu_{+}\nu_{+}$ (or $\nu_{-}\nu_{-}$) may be achieved by introducing a discrete symmetry that gives the difference between $\nu_{+}\nu_{+}$, and $\nu_{-}\nu_{-}$.

It is generally expected in the quasi degenerate mass pattern II that the effective neutrino mass $m_{\beta\beta}$ is larger than $\mathcal{O}(\sqrt{\Delta m_{\text{atm}}^2})$. The predicted $m_{\beta\beta}$ satisfies the mass ordering of

$$m_{\beta\beta}^2 : \Delta m_{\text{atm}}^2 : \Delta m_{\odot}^2 \sim 1 : |\eta| : \eta^2, \tag{116}$$

for C1) with $m_1 \sim m_2 \sim m_3$,

$$m_{\beta\beta}^2 : \Delta m_{\text{atm}}^2 : \Delta m_{\odot}^2 \sim 1 : |\eta| : \eta^2 + \frac{qr'}{2}\varepsilon^2, \tag{117}$$

for C1) with $m_1 \sim m_2 \sim -m_3$, and

$$m_{\beta\beta}^2 : \Delta m_{\text{atm}}^2 : \Delta m_{\odot}^2 \sim 1 : |\eta| : |\eta\varepsilon|, \tag{118}$$

for C2) with $m_1 \sim m_2 \sim \pm m_3$. The mass scale of $m_{\beta\beta}$ is, therefore, given by $\sqrt{\Delta m_{\text{atm}}^2/|\eta|}$. The three figures, FIG.15 for C2) with $m_1 \sim m_2 \sim m_3$ and for C1) and C2) with $m_1 \sim m_2 \sim -m_3$, show the same shape characterized by the rapid rise in $m_{\beta\beta}$ around $|\eta|(\sim |\sin\theta_{13}|) = 0$ as indicated by Eqs.(117) and (118). This behavior generally disappears for C1) because η is not directly related to $\sin\theta_{13}(\sim \varepsilon)$. The texture giving $m_1 \sim m_2 \sim m_3$ shows no rise at $\sin\theta_{13} = 0$. However, the texture giving $m_1 \sim m_2 \sim -m_3$ also shows this rapid rise. It is because η is related to $\sin\theta_{13}$ by Eq.(91). It should be noted that, in textures with $m_1 \sim m_2 \sim -m_3$, the approximate $L_{\mu} - L_{\tau}$ conservation is respected. The results of our calculations turn out to give similar behaviors of $\cos 2\theta_{23}$ and $m_{\beta\beta}$ versus $\sin\theta_{13}$ to those predicted in Ref.[34], which has discussed the neutrino oscillation phenomenology based on the approximate $L_{\mu} - L_{\tau}$ conservation. Namely, $|\cos 2\theta_{23}|$ is proportional to $|\sin\theta_{13}|$ and $m_{\beta\beta}$ rapidly increases as $|\sin\theta_{13}| \rightarrow 0$.

The flavor neutrino masses receive radiative corrections if the neutrino masses are created at relatively higher scale such as 10^{10} TeV. It has been argued that neutrinos in the normal mass hierarchy do not receive large radiative effects, and the form of the texture restores, at low energies, its original one [39]. However, other two mass patterns are likely influenced by these radiative corrections [40]. So, the proposed textures may not be respected by observed neutrinos if they are the textures determined at high energies. Conversely, we should discuss how the textures realized at low energies are evolved into those realized at high energies, which may exhibit some good ordering. Any underlying dynamics that respects the approximate μ - τ symmetry should induce, at low energies, one of our textures because the symmetry structure is not drastically disturbed.

ACKNOWLEDGMENTS

The authors are grateful to I. Aizawa, and T. Kitabayashi for useful discussions. The work of M.Y. is supported by the Grants-in-Aid for Scientific Research on Priority Areas (No 13135219) from the Ministry of Education, Culture, Sports, Science, and Technology, Japan.

APPENDIX A: ESTIMATION OF NEUTRINO MASSES AND MIXING ANGLES

In this Appendix, we show our estimation of neutrino masses and mixing angles discussed in Ref.[22]. This estimation is based on the formula in Ref.[41], where M_ν is parameterized by

$$M_\nu = \begin{pmatrix} M_{ee} & M_{e\mu} & M_{e\tau} \\ M_{e\mu} & M_{\mu\mu} & M_{\mu\tau} \\ M_{e\tau} & M_{\mu\tau} & M_{\tau\tau} \end{pmatrix}. \quad (\text{A1})$$

There is a general formula for deriving mixing angles and masses given by

$$\tan 2\theta_{12} = \frac{2X}{\lambda_2 - \lambda_1}, \quad (\text{A2})$$

$$\tan 2\theta_{13} = \frac{2Y}{\lambda_3 - M_{ee}}, \quad (\text{A3})$$

$$(M_{\tau\tau} - M_{\mu\mu}) \sin 2\theta_{23} - 2M_{\mu\tau} \cos 2\theta_{23} = 2s_{13}X, \quad (\text{A4})$$

and

$$\begin{aligned} m_1 &= c_{12}^2\lambda_1 + s_{12}^2\lambda_2 - 2c_{12}s_{12}X, & m_2 &= s_{12}^2\lambda_1 + c_{12}^2\lambda_2 + 2c_{12}s_{12}X, \\ m_3 &= c_{13}^2\lambda_3 + 2c_{13}s_{13}Y + s_{13}^2M_{ee}, \end{aligned} \quad (\text{A5})$$

where

$$\begin{aligned} X &= \frac{c_{23}M_{e\mu} - s_{23}M_{e\tau}}{c_{13}}, & Y &= s_{23}M_{e\mu} + c_{23}M_{e\tau}, \\ \lambda_1 &= c_{13}^2M_{ee} - 2c_{13}s_{13}Y + s_{13}^2\lambda_3, & \lambda_2 &= c_{23}^2M_{\mu\mu} + s_{23}^2M_{\tau\tau} - 2s_{23}c_{23}M_{\mu\tau}, \\ \lambda_3 &= s_{23}^2M_{\mu\mu} + c_{23}^2M_{\tau\tau} + 2s_{23}c_{23}M_{\mu\tau}. \end{aligned} \quad (\text{A6})$$

By inserting the mass matrix Eq.(4) into these equations, we can calculate neutrino masses and mixing angles for any types of textures. By using Eqs.(A2) and (A6), we derive

$$\Delta m_\odot^2 = \frac{\lambda_2^2 - \lambda_1^2}{\cos 2\theta_{12}}, \quad (\text{A7})$$

which can be transformed into

$$\Delta m_\odot^2 = \frac{2(m_1 + m_2)X}{\sin 2\theta_{12}}, \quad (\text{A8})$$

instead of Eq.(A7) if $\theta_{12} \neq 0$.

For C1), masses and mixing angles are given by

$$\begin{aligned} m_1 &\approx \frac{a + d - \sigma e - (d + \sigma e - a)t_{13}^2 + 2(\sigma e\Delta + \varepsilon d')\Delta}{2} - \frac{X}{\sin 2\theta_{12}}, \\ m_2 &\approx \frac{a + d - \sigma e - (d + \sigma e - a)t_{13}^2 + 2(\sigma e\Delta + \varepsilon d')\Delta}{2} + \frac{X}{\sin 2\theta_{12}}, \\ m_3 &\approx d + \sigma e + (d + \sigma e - a)t_{13}^2 - 2(\sigma e\Delta + \varepsilon d')\Delta, \end{aligned} \quad (\text{A9})$$

and

$$\begin{aligned} \tan 2\theta_{12} &\approx \frac{2X}{d - \sigma e - a + (d + \sigma e - a)t_{13}^2 + 2(\sigma e\Delta + \varepsilon d')\Delta}, \\ \tan 2\theta_{13} &\approx \frac{2Y}{d + \sigma e - a - 2(\sigma e\Delta + \varepsilon d')\Delta}, \\ \cos 2\theta_{23} &\approx 2\Delta, \quad \sin 2\theta_{23} \approx \sigma, \end{aligned} \quad (\text{A10})$$

with

$$X \approx \sqrt{2}(b + \varepsilon b' \Delta), \quad Y \approx \sqrt{2}\sigma(\varepsilon b' - b\Delta), \quad \Delta \approx -\frac{\sigma\varepsilon d' + \sqrt{2}s_{13}b}{2e}, \quad (\text{A11})$$

where we see that $\sin \theta_{13} \rightarrow 0$ as $\varepsilon \rightarrow 0$. For C2), masses and mixing angles are given by

$$\begin{aligned} m_1 &\approx \frac{a + d + \sigma e - (d - \sigma e - a)t_{13}^2 - 2(\sigma e\Delta - \varepsilon d')\Delta}{2} - \frac{X}{\sin 2\theta_{12}}, \\ m_2 &\approx \frac{a + d + \sigma e - (d - \sigma e - a)t_{13}^2 - 2(\sigma e\Delta - \varepsilon d')\Delta}{2} + \frac{X}{\sin 2\theta_{12}}, \\ m_3 &\approx d - \sigma e + (d - \sigma e - a)t_{13}^2 + 2(\sigma e\Delta - \varepsilon d')\Delta, \end{aligned} \quad (\text{A12})$$

and

$$\begin{aligned} \tan 2\theta_{12} &\approx \frac{2X}{d + \sigma e - a + (d - \sigma e - a)t_{13}^2 - 2(\sigma e\Delta - \varepsilon d')\Delta}, \\ \tan 2\theta_{13} &\approx \frac{2Y}{d - \sigma e - a + 2(\sigma e\Delta - \varepsilon d')\Delta}, \\ \cos 2\theta_{23} &\approx 2\Delta, \quad \sin 2\theta_{23} \approx -\sigma, \end{aligned} \quad (\text{A13})$$

with

$$X \approx \sqrt{2}(\varepsilon b' + b\Delta), \quad Y \approx -\sqrt{2}\sigma(b - \varepsilon b'\Delta), \quad \Delta \approx \frac{\sigma d' - \sqrt{2}s_{13}b'}{2e + \sqrt{2}s_{13}b}, \quad (\text{A14})$$

where we see that $\sin \theta_{12} \rightarrow 0$ as $\varepsilon \rightarrow 0$. It should be stressed again that the smallness of $\sin^2 \theta_{13}$ is not guaranteed by the μ - τ symmetry because Y is mainly proportional to b . To obtain its smallness needs an additional requirement.

From Eqs.(A11) and (A14), we can obtain that

$$s_{13} \approx \frac{2eb' + \sigma bd'}{\sqrt{2}[\sigma e(d + \sigma e - a) - b^2]}\varepsilon, \quad \cos 2\theta_{23} \approx -\frac{(d + \sigma e - a)d' + 2bb'}{\sigma e(d + \sigma e - a) - b^2}\varepsilon, \quad (\text{A15})$$

for $d + \sigma e - a \neq 0$, from Eq.(A10) for C1), and

$$s_{13} \approx -\frac{2\sqrt{2}eb - \varepsilon^2 b'd'}{2\sigma e(d - \sigma e - a)}, \quad \cos 2\theta_{23} \approx \frac{(d - \sigma e - a)d' + 2bb'}{\sigma e(d - \sigma e - a) - b^2}\varepsilon, \quad (\text{A16})$$

for $d - \sigma e - a \neq 0$, from Eq.(A13) for C2). Since $b \sim 0$ in C2), $\cos 2\theta_{23}$ is further reduced to

$$\cos 2\theta_{23} \approx \frac{\sigma d'}{e}\varepsilon. \quad (\text{A17})$$

-
- [1] B. Pontecorvo, Sov. Phys. JETP **7** (1958) 172 [Zh. Eksp. Teor. Fiz. **34** (1958) 247]; Z. Maki, M. Nakagawa and S. Sakata, Prog. Theor. Phys. **28** (1962) 870.
 - [2] Y. Fukuda *et al.*, [Super-Kamiokande Collaboration], Phys. Rev. Lett. **81** (1998) 1562; Phys. Rev. Lett. **82** (1999) 2430; T. Kajita for the collaboration, Nucl. Phys. Proc. Suppl. **77** (1999) 123. See also, T. Kajita and Y. Totsuka, Rev. Mod. Phys. **73** (2001) 85; A. Suzuki, “Evidence for Neutrino Mass”, Talk given at *Neutrino 2006: The XXII International Conference on Neutrino Physics and Astrophysics*, Santa Fe, New Mexico, USA (June 13-19, 2006).
 - [3] Y. Suzuki, “Accelerator and Atmospheric Neutrinos”, Talk given at *XXII International Symposium on Lepton-Photon Interactions at High Energy*, Uppsala, Sweden (June 30-July 5, 2005); A. Poon, “Solar and Reactor Neutrinos”, Talk given at *XXII International Symposium on Lepton-Photon Interactions at High Energy*, Uppsala, Sweden (June 30-July 5, 2005);
 - [4] J.N. Bahcall, W.A. Fowler, I. Iben and R.L. Sears, Astrophys. J. **137** (1963) 344; J. Bahcall, Phys. Rev. Lett. **12** (1964) 300; R. Davis, Jr., Phys. Rev. Lett. **12** (1964) 303; R. Davis, Jr., D.S. Harmer and K.C. Hoffman, Phys. Rev. Lett. **20** (1968) 1205; J.N. Bahcall, N.A. Bahcall and G. Shaviv, Phys. Rev. Lett. **20** (1968) 1209; J.N. Bahcall and R. Davis, Jr., Science **191** (1976) 264.

- [5] Y. Fukuda *et al.*, [Super-Kamiokande Collaboration], Phys. Rev. Lett. **81** (1998) 1158; [Erratum-ibid **81** (1998) 4297]; B.T. Cleveland *et al.*, Astrophys. J. **496** (1998) 505; W. Hampel *et al.*, [GNO Collaboration], Phys. Lett. B **447** (1999) 1271; Q.A. Ahmed *et al.*, [SNO Collaboration], Phys. Rev. Lett. **87** (2001) 071301; Phys. Rev. Lett. **89** (2002) 011301.
- [6] S. H. Ahn, *et al.*, [K2K Collaboration], Phys. Lett. B **511** (2001) 178; Phys. Rev. Lett. **90** (2003) 041801.
- [7] M. Apollonio, *et al.*, [CHOOZ Collaboration], Euro. Phys. J. C **27** (2003) 331; K. Eguchi, *et al.*, [KamLAND collaboration], Phys. Rev. Lett. **90** (2003) 021802; K. Inoue, [KamLAND collaboration], New. J. Phys. **6** (2004) 147.
- [8] T. Yanagida, in *Proceedings of the Workshop on Unified Theories and Baryon Number in the Universe* edited by A. Sawada and A. Sugamoto (KEK Report No.79-18, Tsukuba, 1979), p.95; Prog. Theor. Phys. **64** (1980) 1103; M. Gell-Mann, P. Ramond and R. Slansky, in *Supergravity* edited by P. van Nieuwenhuizen and D.Z. Freedmann (North-Holland, Amsterdam 1979), p.315; R.N. Mohapatra and G. Senjanović, Phys. Rev. Lett. **44** (1980) 912. See also, P. Minkowski, Phys. Lett. **B67** (1977) 421.
- [9] R.N. Mohapatra and G. Senjanović, Phys. Rev. D **23** (1981) 165; C. Wetterich, Nucl. Phys. B **187** (1981) 343. See also, J. Schechter and J.W.F. Valle, Phys. Rev. D **22** (1980) 2227.
- [10] A. Zee, Phys. Lett. **93B** (1980) 389; Phys. Lett. **161B** (1985) 141; L. Wolfenstein, Nucl. Phys. B **175** (1980) 93; S. T. Petcov, Phys. Lett. **115B** (1982) 401.
- [11] A. Zee, Nucl. Phys. **264B** (1986) 99; K. S. Babu, Phys. Lett. B **203** (1988) 132; D. Chang, W-Y. Keung and P.B. Pal, Phys. Rev. Lett. **61** (1988) 2420; J. Schechter and J.W.F. Valle, Phys. Lett. B **286** (1992) 321.
- [12] G.L. Fogli, E. Lisi, A. Marrone, A. Palazzo, Prog. Part. Nucl. Phys. **57** (2006) 742. See also, S. Goswami, A. Bandyopadhyay and S. Choubey, Nucl. Phys. Proc. Suppl. **143** (2005) 121; G. Altarelli, Nucl. Phys. Proc. Suppl. **143** (2005) 470; A. Bandyopadhyay, Phys. Lett. B **608** (2005) 115.
- [13] O. Mena and S. Parke, Phys. Rev. D **69** (2004) 117301.
- [14] See for example, R. N. Mohapatra and A. Y. Smirnov, “Neutrino Mass and New Physics”, [arXiv: hep-ph/0603118] (to be published in the Annual Review of Nuclear and Particle Science Vol. 56 (2006)). See also, R. Peccei, “Physics Beyond the Standard Model - What we know, don’t know, and what it means for neutrinos”, Talk given at *Neutrino 2006: The XXII International Conference on Neutrino Physics and Astrophysics*, Santa Fe, New Mexico, USA (June 13-19, 2006); R.N. Mohapatra, “Models of Neutrino Mass”, Talk given at *Neutrino 2006: The XXII International Conference on Neutrino Physics and Astrophysics*, Santa Fe, New Mexico, USA (June 13-19, 2006).
- [15] T. Fukuyama and H. Nishiura, in *Proceedings of International Workshop on Masses and Mixings of Quarks and Leptons* edited by Y. Koide (World Scientific, Singapore, 1997), p.252; “Mass Matrix of Majorana Neutrinos”, [arXiv:hep-ph/9702253]; Y. Koide, H. Nishiura, K. Matsuda, T. Kikuchi and T. Fukuyama, Phys. Rev. D **66** (2002) 093006; Y. Koide, Phys. Rev. D **69** (2004) 093001; K. Matsuda and H. Nishiura, Phys. Rev. D **69** (2004) 117302; Phys. Rev. D **71** (2005) 073001; Phys. Rev. D **72** (2005) 033011; Phys. Rev. D **73** (2006) 013008.
- [16] R.N. Mohapatra and S. Nussinov, Phys. Rev. D **60** (1999) 013002; C.S. Lam, Phys. Lett. B **507** (2001) 214; Phys. Rev. D **71** (2005) 093001; Z.Z. Xing, Phys. Rev. D **61** (2000) 057301; Phys. Rev. D **64** (2001) 093013; “Neutrino Telescopes as a Probe of Broken μ - τ Symmetry”, [arXiv: hep-ph/0605219]; “Nearly Tri-bimaximal Neutrino Mixing and CP Violation from μ - τ Symmetry Breaking”, [arXiv: hep-ph/0607091]; E. Ma and M. Raidal, Phys. Rev. Lett. **87** (2001) 011802; [Erratum-ibid **87** (2001) 159901]; A. Datta and P.J. O’Donnell, Phys. Rev. D **72** (2005) 113002; Y.H. Ahn, S.K. Kang, C.S. Kim and J. Lee, Phys. Rev. D **73** (2006) 093005.
- [17] T. Kitabayashi and M. Yasuè, Phys. Lett. B **524** (2002) 308; Int. J. Mod. Phys. A **17** (2002) 2519; Phys. Rev. D **67** (2003) 015006; I. Aizawa, M. Ishiguro, T. Kitabayashi and M. Yasuè, Phys. Rev. D **70** (2004) 015011; I. Aizawa, T. Kitabayashi and M. Yasuè, Phys. Rev. D **71** (2005) 075011.
- [18] W. Grimus and L. Lavoura, JHEP **0107** (2001) 045; Euro. Phys. J. C **28** (2003) 123; Phys. Lett. B **572** (2003) 189; Phys. Lett. B **579** (2004) 113; J. Phys. G **30** (2004) 1073; JHEP **0508** (2005) 013; W. Grimus, A.S. Joshipura, S. Kaneko, L. Lavoura and M. Tanimoto, JHEP **0407** (2004) 078; W. Grimus, A.S. Joshipura, S. Kaneko, L. Lavoura, H. Sawanaka and M. Tanimoto, Nucl. Phys. B **713** (2005) 151; W. Grimus, S. Kaneko, L. Lavoura, H. Sawanaka and M. Tanimoto, JHEP **0601** (2006) 110.
- [19] R.N. Mohapatra, JHEP **0410** (2004) 027; R.N. Mohapatra and S. Nasri, Phys. Rev. D **71** (2005) 033001; R.N. Mohapatra, S. Nasri and Hai-Bo Yu, Phys. Lett. B **615** (2005) 231; Phys. Rev. D **72** (2005) 033007; Phys. Lett. B **639** (2006) 318.
- [20] T. Kitabayashi and M. Yasue, Phys. Lett. B **524** (2002) 308 in Ref.[17]; I. Aizawa, M. Ishiguro, T. Kitabayashi and M. Yasuè, in Ref.[17].
- [21] M. Frigerio and A.Yu. Smirnov, Nucl. Phys. B **640** (2002) 233; R.N. Mohapatra and W. Rodejohann, Phys. Rev. D **72** (2005) 053001.
- [22] K. Fuki and M. Yasuè, Phys. Rev. D **73** (2006) 055014.
- [23] W. Grimus, A.S. Joshipura, S. Kaneko, L. Lavoura, H. Sawanaka and M. Tanimoto, in Ref.[18].
- [24] A. de Gouvêa, Phys. Rev. D **69** (2004) 093007.
- [25] R.N. Mohapatra, in Ref.[19]; W. Grimus, A.S. Joshipura, S. Kaneko, L. Lavoura, H. Sawanaka and M. Tanimoto, in Ref.[18]; R.N. Mohapatra and W. Rodejohann, in Ref.[21]; F. Plentinger and W. Rodejohann, Phys. Lett. B **625** (2005) 264. See also, A. Joshipura, “Summary of Model Predictions for U_{e3} ”, Talk given at the *5th Workshop on “Neutrino Oscillations and their Origin (NOON2004)*, Tokyo, Japan (February 11-15, 2004), [arXiv:hep-ph/0411154].
- [26] Riazuddin, JHEP **0310** (2003) 009.
- [27] For a review, see for example, R. N. Mohapatra and A. Y. Smirnov, in [14].
- [28] See for example, W. Grimus and L. Lavoura, JHEP **0107** (2001) 045, Euro. Phys. J. C **28** (2003) 123, and J. Phys. G **30** (2004) 73 in Ref.[18]; E. Ma and G. Rajasekaran, Phys. Rev. D **68** (2003) 071302; R.N. Mohapatra, in Ref.[19]; A. Joshipura, “Universal 2-3 symmetry”, [arXiv: hep-ph/0512252]; K. Matsuda and H. Nishiura, in Ref.[15]; W. Grimus,

- A.S. Joshipura, S. Kaneko, L. Lavoura, H. Sawanaka and M. Tanimoto, in Ref.[18].
- [29] For recent studies, see for example, R.N. Mohapatra, S. Nasri and Hai-Bo Yu, Phys. Lett. B **636** (2006) 114; N. Haba and W. Rodejohann, Phys. Rev. D **74** (2006) 017701.
 - [30] I. Aizawa and M. Yasuè, Phys. Rev. D **73** (2006) 015002.
 - [31] See for example, B. Adhikary, “Soft Breaking of L_μ - L_τ Symmetry: Light Neutrino Spectrum and Leptogenesis”, [arXiv: hep-ph/0604009].
 - [32] See for example, S. Pascoli and S.T. Petcov, Nucl. Phys. Proc. Suppl. **138** (2005) 233; S. Pascoli, S.T. Petcov and T. Schwetz, Nucl. Phys. B **734** (2005) 24; M. Hirsch, E. Ma, J.W.F. Valle and A.V. del Moral, Phys. Rev. D **72** (2005) 091301; [Erratum-ibid **72** (2005) 119904]; M. Hirsch, “Phenomonology of Double Beta Decay”, Talk given at *Neutrino 2006: The XXII International Conference on Neutrino Physics and Astrophysics*, Santa Fe, New Mexico, USA (June 13-19, 2006).
 - [33] A. Merle and W. Rodejohann, Phys. Rev. D **73** (2006) 073012.
 - [34] S. Choubey and W. Rodejohann, Euro. Phys. J. C **40** (2005) 259.
 - [35] B. Adhikary, in Ref.[31]; T. Ota and W. Rodejohann, Phys. Lett. B **639** (2006) 322. See also, X. G. He et al., Phys. Rev. D **43** (1991) 22; Phys. Rev. D **44** (1991) 2118; E. Ma, D. P. Roy and S. Roy, Phys. Lett. B **525** (2002) 101.
 - [36] See for example, C. Giunti, Acta. Phys. Pol. B **36** (2005) 3215.
 - [37] H.V. Klapdor-Kleingrothaus *et al.*, Euro. Phys. J. A **12** (2001) 147.
 - [38] See for example, S. Elliott, “Intro to experimental program” Talk given at *Neutrino 2006: The XXII International Conference on Neutrino Physics and Astrophysics*, Santa Fe, New Mexico, USA (June 13-19, 2006).
 - [39] See for example, S. Antusch, J. Kersten, M. Lindner and M. Ratz, Nucl. Phys. B **674** (2003) 401; S. Antusch, J. Kersten, M. Lindner, M. Ratz and M.A. Schmidt, JHEP **0503** (2005) 024.
 - [40] For recent studies, see for example, R.N. Mohapatra, M.K. Parida and G. Rajasekaran, Phys. Rev. D **71** (2005) 057301; J.W. Mei, Phys. Rev. D **71** (2005) 073012; S. Luo, J.W. Mei and Z.Z. Xing, Phys. Rev. D **72** (2005) 053014; S. Luo and Z.Z. Xing, Phys. Lett. B **632** (2006) 341.
 - [41] I. Aizawa, T. Kitabayashi and M. Yasuè, in Ref.[17].

TABLE I: The textures consistent with the observed results, where the overall scale d_0 is omitted, $\sin \theta_{13} = 0$ ($\sin \theta_{12} = 0$) corresponds to textures with $s_{23} \approx \sigma/\sqrt{2}$ ($s_{23} \approx -\sigma/\sqrt{2}$) for $\sigma = \pm 1$, and $R = \Delta m_{\odot}^2/\Delta m_{atm}^2$. In the quasi degenerate mass pattern II, the estimate of the effective neutrino mass $m_{\beta\beta}$ is shown. In some textures, the constraint on η arises to yield $\tan 2\theta_{12} = \mathcal{O}(1)$ as shown in the each texture's last line if it is required.

C1) $\sin \theta_{13} = 0$	C2) $\sin \theta_{12} = 0$
Normal Mass Hierarchy	
$\begin{pmatrix} p\eta & \eta + \varepsilon & -\sigma(\eta - \varepsilon) \\ \eta + \varepsilon & 1 + r'\varepsilon & \sigma(1 - s\eta) \\ -\sigma(\eta - \varepsilon) & \sigma(1 - s\eta) & 1 - r'\varepsilon \end{pmatrix}$ $\cos 2\theta_{23} \approx -\sqrt{2}\sigma r' \sin \theta_{13}$ $R \approx \frac{s+p}{\sqrt{2}\sin 2\theta_{12}} \eta^2$ $(*) \eta \gg \varepsilon^2$	$\begin{pmatrix} p\eta & \eta + \varepsilon & -\sigma(\eta - \varepsilon) \\ \eta + \varepsilon & 1 + r'\varepsilon & -\sigma(1 - s\eta) \\ -\sigma(\eta - \varepsilon) & -\sigma(1 - s\eta) & 1 - r'\varepsilon \end{pmatrix}$ $\cos 2\theta_{23} \approx \frac{\sigma(s-p)r' \tan 2\theta_{12}}{2} \sin \theta_{13}$ $R \approx \frac{s^2-p^2}{2\cos 2\theta_{12}} \sin^2 \theta_{13}$ $(*) \eta \sim \varepsilon $
Inverted Mass Hierarchy	
$\begin{pmatrix} 2-p\eta & \eta + \varepsilon & -\sigma(\eta - \varepsilon) \\ \eta + \varepsilon & 1 + r'\varepsilon & -\sigma(1 - s\eta) \\ -\sigma(\eta - \varepsilon) & -\sigma(1 - s\eta) & 1 - r'\varepsilon \end{pmatrix}$ $\cos 2\theta_{23} \approx -\sqrt{2}\sigma r' \sin \theta_{13}$ $R \approx \frac{2\sqrt{2}}{\sin 2\theta_{12}} (\eta + r' \sin^2 \theta_{13})$ $(*) m_1 \sim m_2$	$\begin{pmatrix} 2-p\eta & \eta + \varepsilon & -\sigma(\eta - \varepsilon) \\ \eta + \varepsilon & 1 + r'\varepsilon & \sigma(1 - s\eta) \\ -\sigma(\eta - \varepsilon) & \sigma(1 - s\eta) & 1 - r'\varepsilon \end{pmatrix}$ $\cos 2\theta_{23} \approx \frac{\sigma(p-s)r' \tan 2\theta_{12}}{2} \sin \theta_{13}$ $R \approx \frac{\sqrt{2}\sigma(p-s)}{\cos 2\theta_{12}} \sin \theta_{13}$ $(*) \eta \sim \varepsilon , m_1 \sim m_2$
$\begin{pmatrix} -(2-\eta) & q + \varepsilon & -\sigma(q - \varepsilon) \\ q + \varepsilon & 1 + r'\varepsilon & -\sigma \\ -\sigma(q - \varepsilon) d_0 & -\sigma & 1 - r'\varepsilon \end{pmatrix}$ $\cos 2\theta_{23} \approx \frac{2\sqrt{2}\sigma(q+r')}{2-qr'} \sin \theta_{13}$ $R \sim \sin^2 \theta_{13} \text{ for } \eta=0$ $(*) m_1 \sim -m_2$...
Quasi Degenerate Mass Pattern I ($ m_{1,2,3} \sim \sqrt{\Delta m_{atm}^2}$)	
$\begin{pmatrix} -(2-\eta) & q + \varepsilon & -\sigma(q - \varepsilon) \\ q + \varepsilon & 1 - r + r'\varepsilon & -\sigma(1 + r) \\ -\sigma(q - \varepsilon) & -\sigma(1 + r) & 1 - r - r'\varepsilon \end{pmatrix}$ $\cos 2\theta_{23} \approx \frac{2\sqrt{2}\sigma[q+r'(1-r)]}{2+2r-qr'} \sin \theta_{13}$ $R \sim \sin^2 \theta_{13} \text{ for } \eta=0$ $(*) r \cos 2\theta_{12} \sim 1, m_1 \sim -m_2$...
Quasi Degenerate Mass Pattern II ($m_{1,2,3}^2 \gg \Delta m_{atm}^2$ and $\kappa = \eta/ \eta $)	
$\begin{pmatrix} 1-\eta & (q\eta + \varepsilon)\eta & -\sigma(q\eta - \varepsilon)\eta \\ (q\eta + \varepsilon)\eta & 1 + r'\varepsilon\eta & \sigma(1 - s\eta)\eta \\ -\sigma(q\eta - \varepsilon)\eta & \sigma(1 - s\eta)\eta & 1 - r'\varepsilon\eta \end{pmatrix}$ $0.07 \lesssim m_{\beta\beta} \lesssim 0.50 \text{ eV}$ $\cos 2\theta_{23} \approx -\sqrt{2}\sigma r' \sin \theta_{13}$ $R \approx \frac{\sqrt{2}\kappa}{\sin 2\theta_{12}} (q\eta - r' \sin^2 \theta_{13})$ $(*) m_1 \sim m_2 \sim m_3$	$\begin{pmatrix} 1-\eta & (q\eta + \varepsilon)\eta & -\sigma(q\eta - \varepsilon)\eta \\ (q\eta + \varepsilon)\eta & 1 + r'\varepsilon\eta & -\sigma(1 - s\eta)\eta \\ -\sigma(q\eta - \varepsilon)\eta & -\sigma(1 - s\eta)\eta & 1 - r'\varepsilon\eta \end{pmatrix}$ $0.07 \leq m_{\beta\beta} \lesssim 0.35 \text{ eV}$ $\cos 2\theta_{23} \approx \frac{\sigma r' s \tan 2\theta_{12}}{4q} \sin \theta_{13}$ $R \approx -\frac{\sqrt{2}\sigma\kappa s}{4q \cos 2\theta_{12}} \sin \theta_{13}$ $(*) \eta \sim \varepsilon , m_1 \sim m_2 \sim m_3$
$\begin{pmatrix} 1+\eta & q\eta^2 + \varepsilon & -\sigma(q\eta^2 - \varepsilon) \\ q\eta^2 + \varepsilon & \eta + r'\varepsilon & -\sigma \\ -\sigma(q\eta^2 - \varepsilon) & -\sigma & \eta - r'\varepsilon \end{pmatrix}$ $0.07 \leq m_{\beta\beta} \lesssim 0.50 \text{ eV}$ $\cos 2\theta_{23} \approx -\sqrt{2}\sigma r' \sin \theta_{13}$ $R \approx \frac{\sqrt{2}}{\sin 2\theta_{12}} \left(q \eta + \frac{r'}{ \eta } \sin^2 \theta_{13} \right)$ $(*) m_1 \sim m_2 \sim -m_3$	$\begin{pmatrix} 1+\eta & (q + \varepsilon)\eta & -\sigma(q - \varepsilon)\eta \\ (q + \varepsilon)\eta & \eta + r'\varepsilon & \sigma \\ -\sigma(q - \varepsilon)\eta & \sigma & \eta - r'\varepsilon \end{pmatrix}$ $0.07 \leq m_{\beta\beta} \lesssim 0.50 \text{ eV}$ \dots $R \approx \frac{\kappa(qr' - 2)}{\sqrt{2}r' \sin 2\theta_{12}} \cos 2\theta_{23}$ $(*) \eta \sim \varepsilon , m_1 \sim m_2 \sim -m_3$

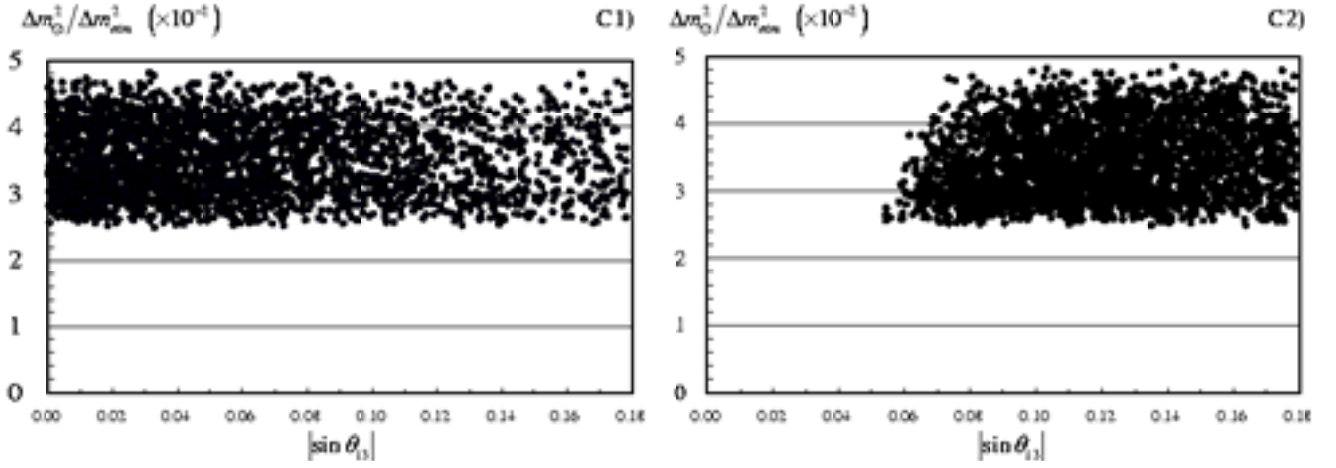


FIG. 1: The predictions of $\Delta m_{\odot}^2/\Delta m_{atm}^2$ as function of $|\sin \theta_{13}|$ for C1) and C2) in the normal mass hierarchy, where $m_{1,2} > 0$ are taken and the experimental upper and lower bounds are applied.

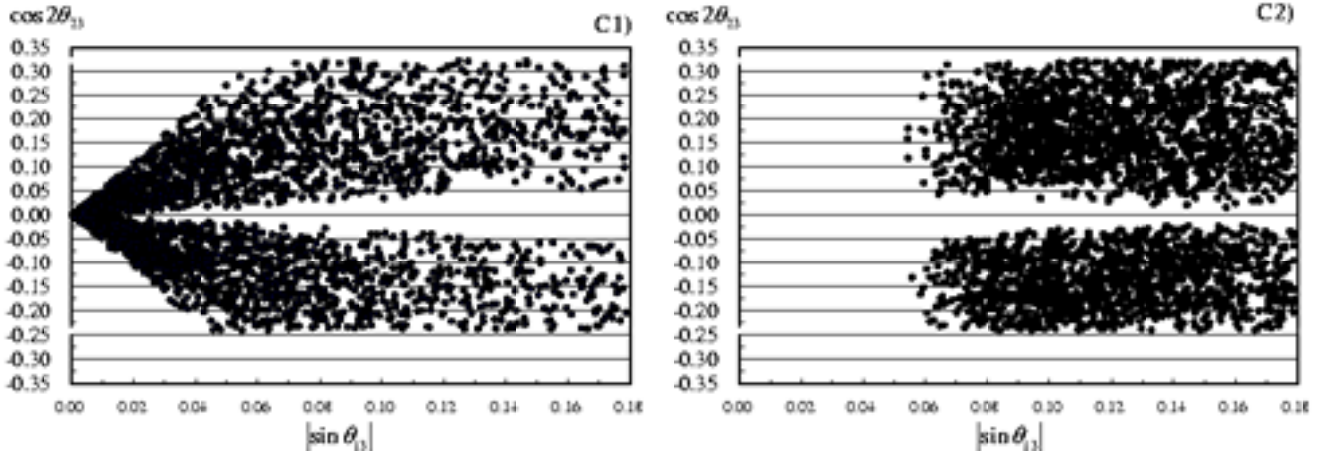


FIG. 2: The same as in FIG.1 but for $\cos 2\theta_{23}$.

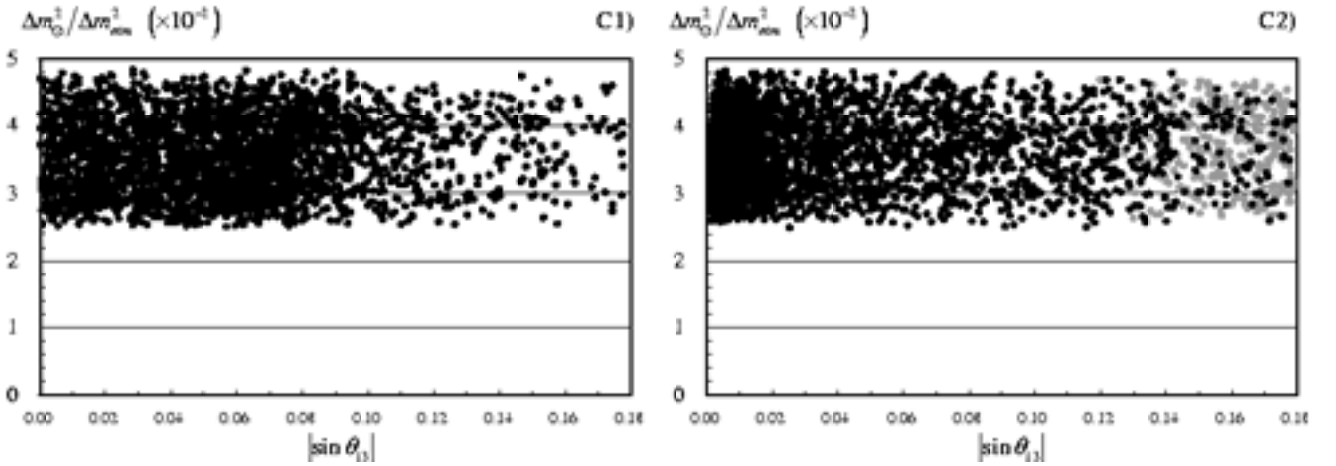
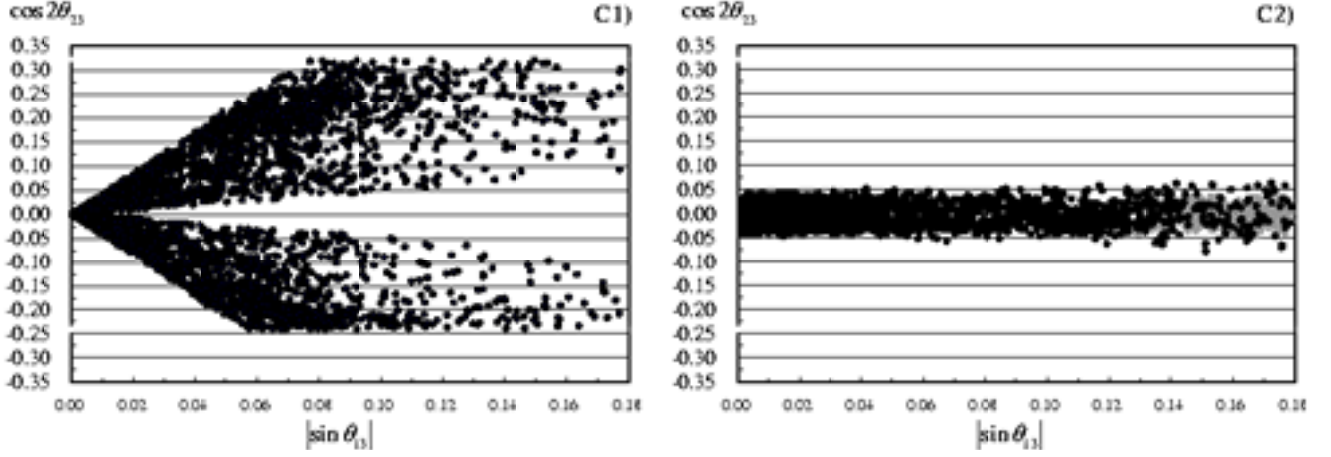
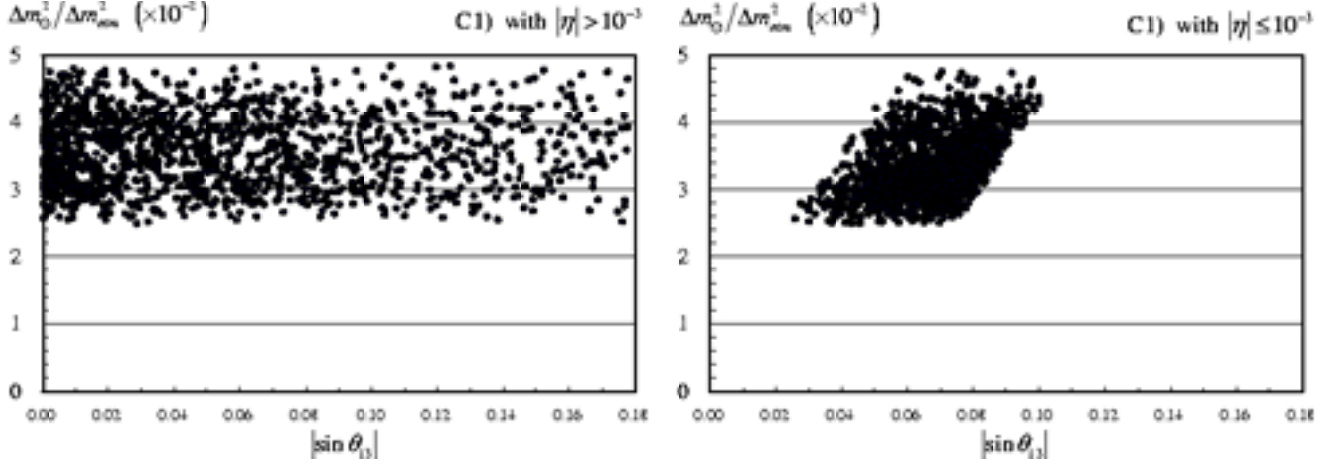
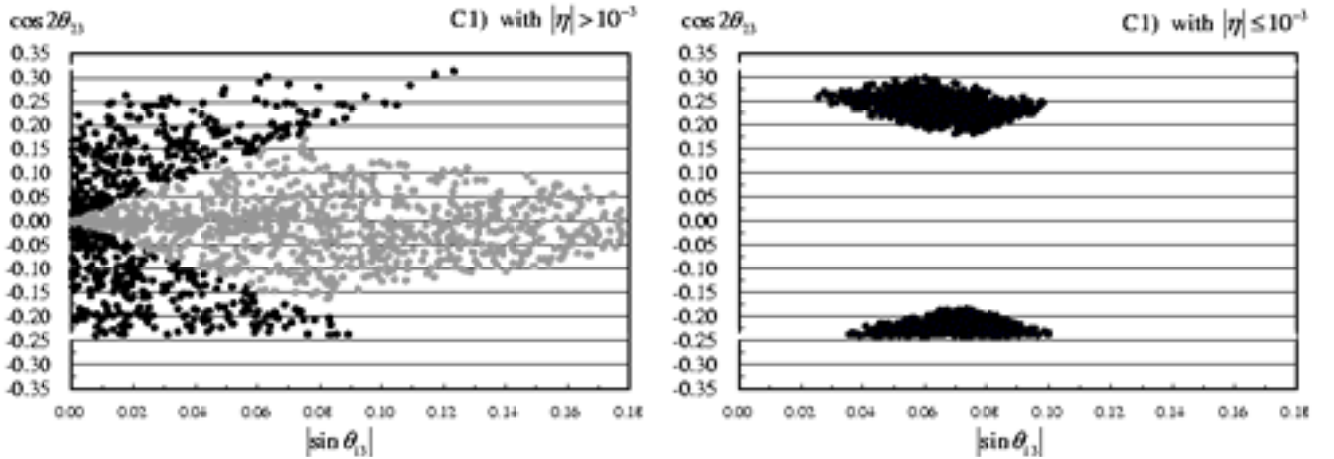


FIG. 3: The same as in FIG.1 but in the inverted mass hierarchy with $m_1 \approx m_2$, where the grey dots in the right figure represents the region of $|\eta| > 1/3$, which lies beyond the approximation due to $\eta^2 \ll 1$.

FIG. 4: The same as in FIG.3 but for $\cos 2\theta_{23}$ FIG. 5: The same as in FIG.1 but in the inverted mass hierarchy for C1) with $m_1 \approx -m_2$, where two regions of $|\eta| > 0.001$ and $|\eta| \leq 0.001$ are separately shown.FIG. 6: The same as in FIG.5 but for $\cos 2\theta_{23}$, where the black (grey) dots in the left figure correspond to $r'q > 0$ ($r'q < 0$).

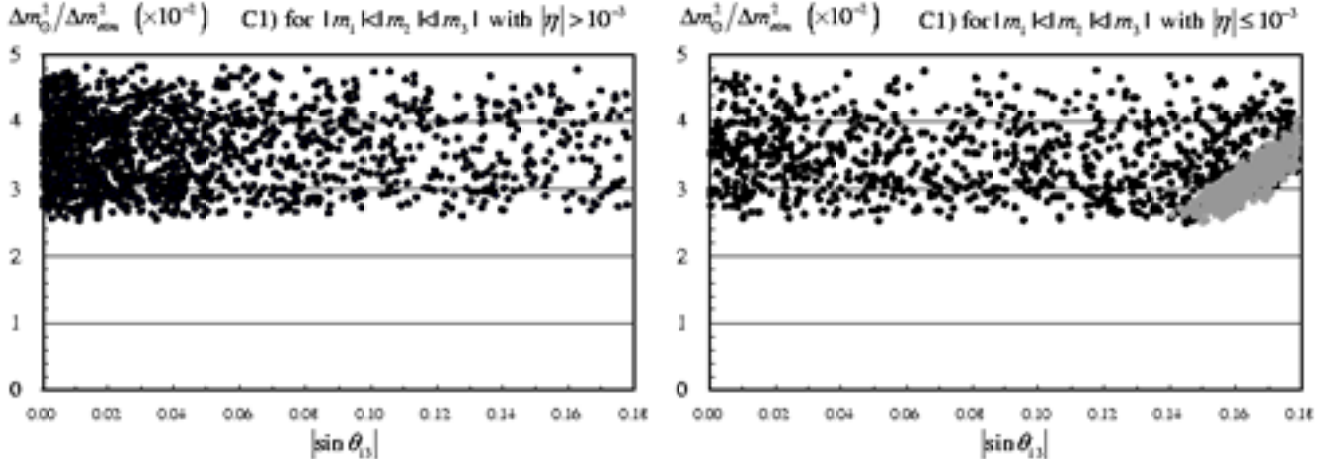


FIG. 7: The same as in FIG.1 but in the quasi degenerate mass pattern I for C1) with the normal mass ordering $|m_1| < |m_2| < |m_3|$, where two regions of $|\eta| > 0.001$ and $|\eta| \leq 0.001$ are separately shown. The black (grey) dots in the right figure correspond to $r' > 0$ ($r' < 0$).

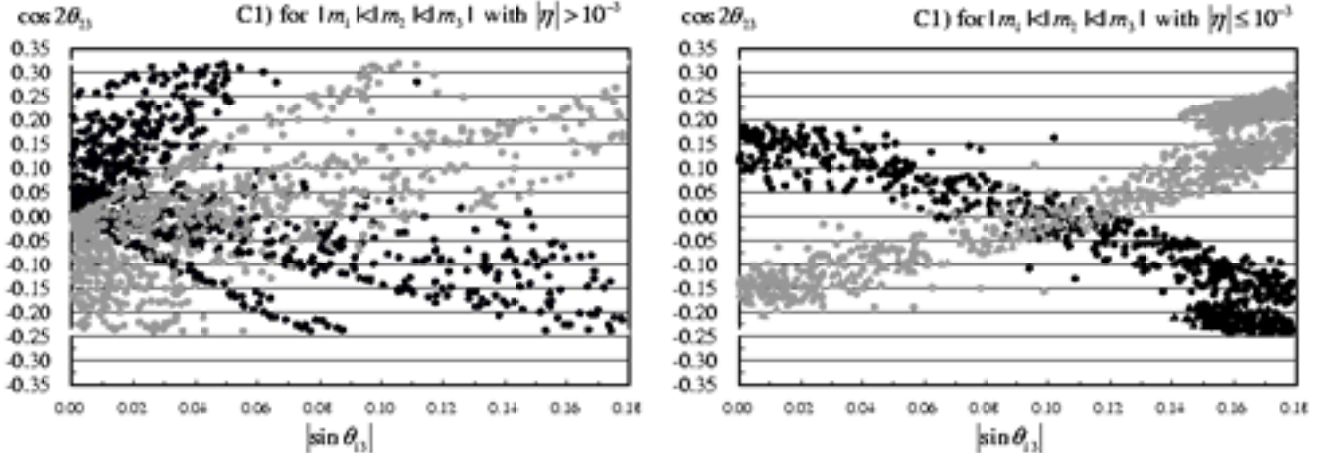


FIG. 8: The same as in FIG.7 but for $\cos 2\theta_{23}$, where the black (grey) marks correspond to $\epsilon > 0$ ($\epsilon < 0$) and, in the right figure, the dots (triangle marks for $|\sin \theta_{13}| \geq 0.14$ and $0.17 \leq |\cos 2\theta_{23}| \leq 0.28$) correspond to $r' > 0$ ($r' < 0$).

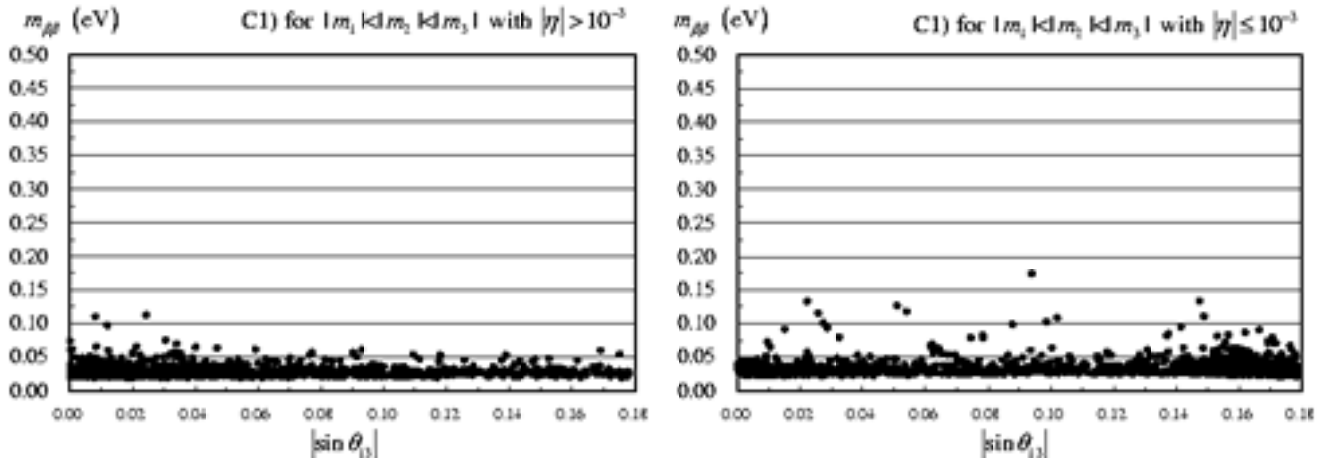


FIG. 9: The same as in FIG.7 but for $m_{\beta\beta}$.

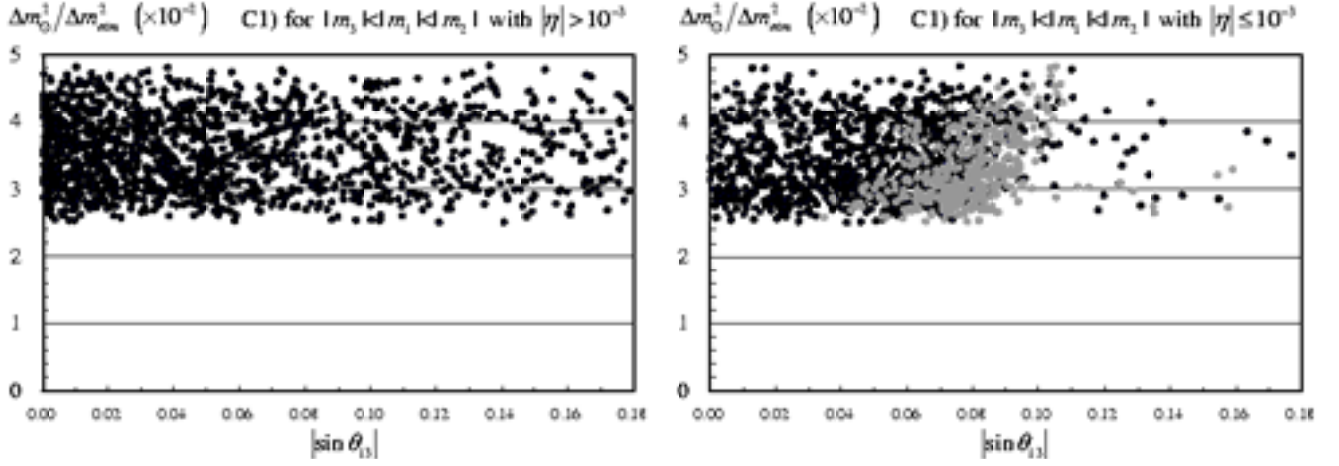


FIG. 10: The same as in FIG.7 but with the inverted mass ordering $|m_3| < |m_1| < |m_2|$, where the black (grey) dots in the right figure correspond to $r > 0$ ($r < 0$).

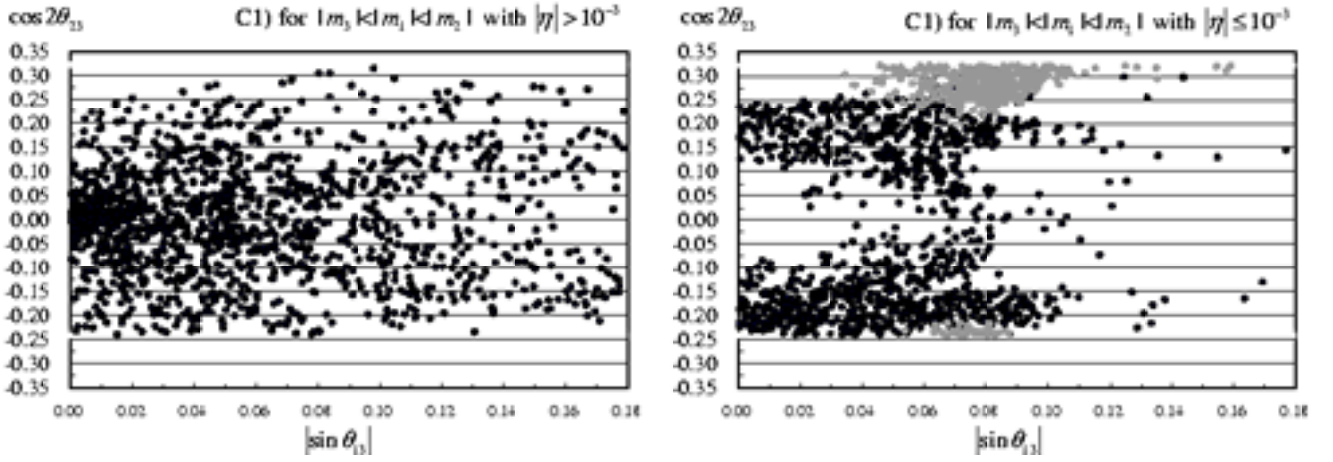


FIG. 11: The same as in FIG.10 but for $\cos 2\theta_{23}$.

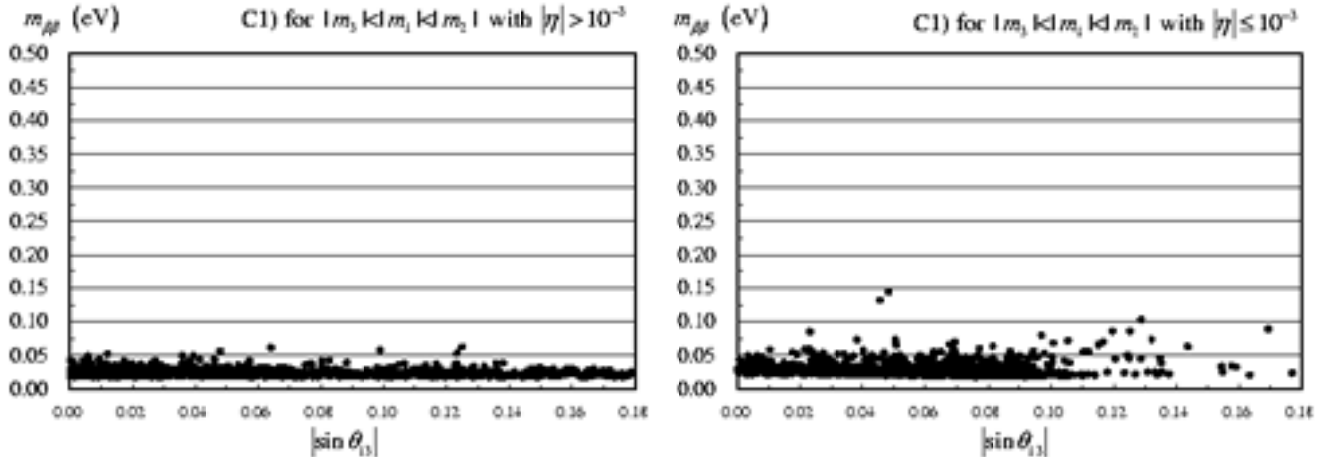


FIG. 12: The same as in FIG.10 but for $m_{\beta\beta}$.

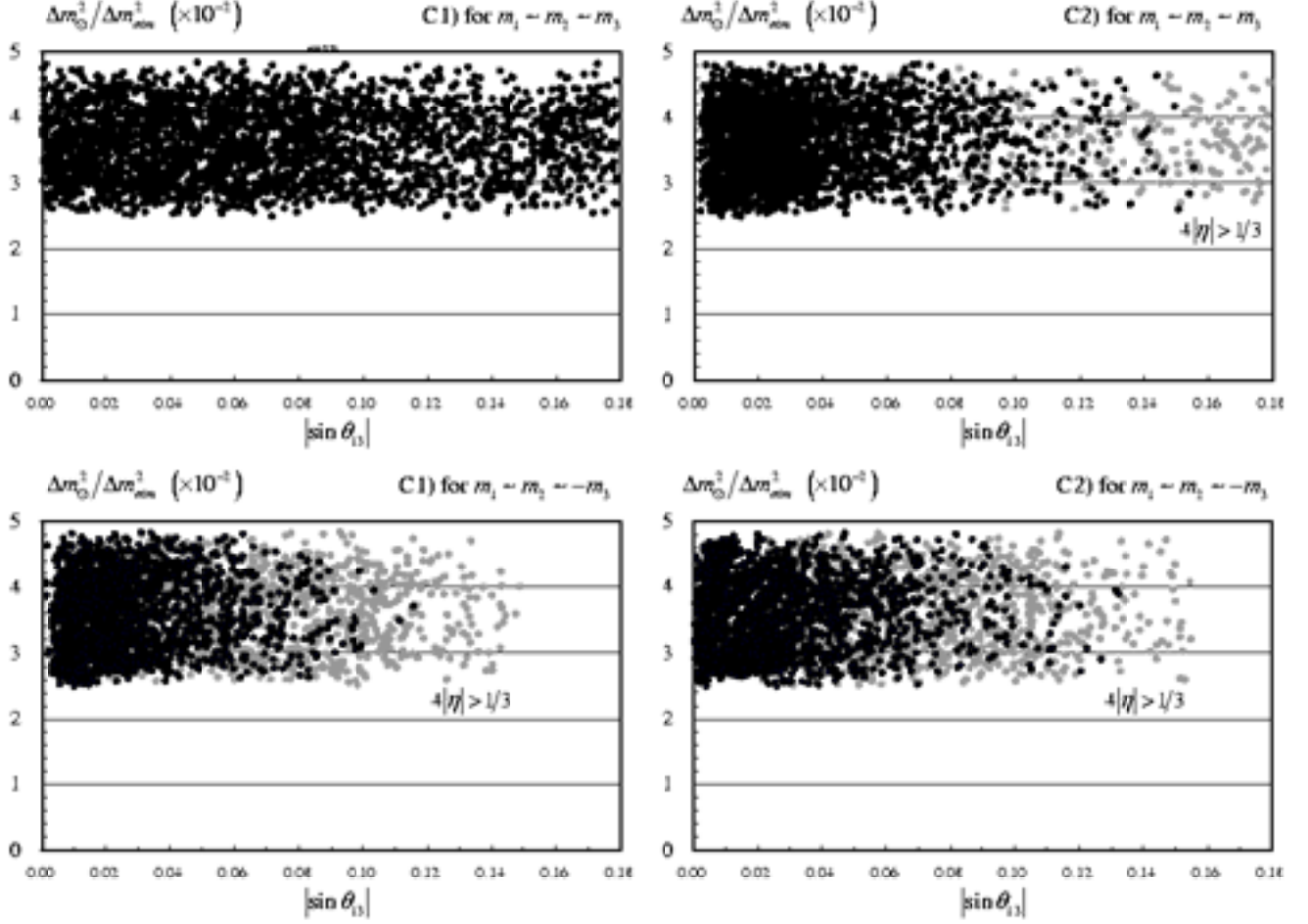


FIG. 13: The same as in FIG.1 but for the quasi degenerate mass pattern II either with $m_1 \sim m_2 \sim m_3$ or $m_1 \sim m_2 \sim -m_3$, where the grey dots represent the region with $4|\eta| > 1/3$, which disturbs the condition $m_{1,2,3}^2 \gg \Delta m_{atm}^2$.

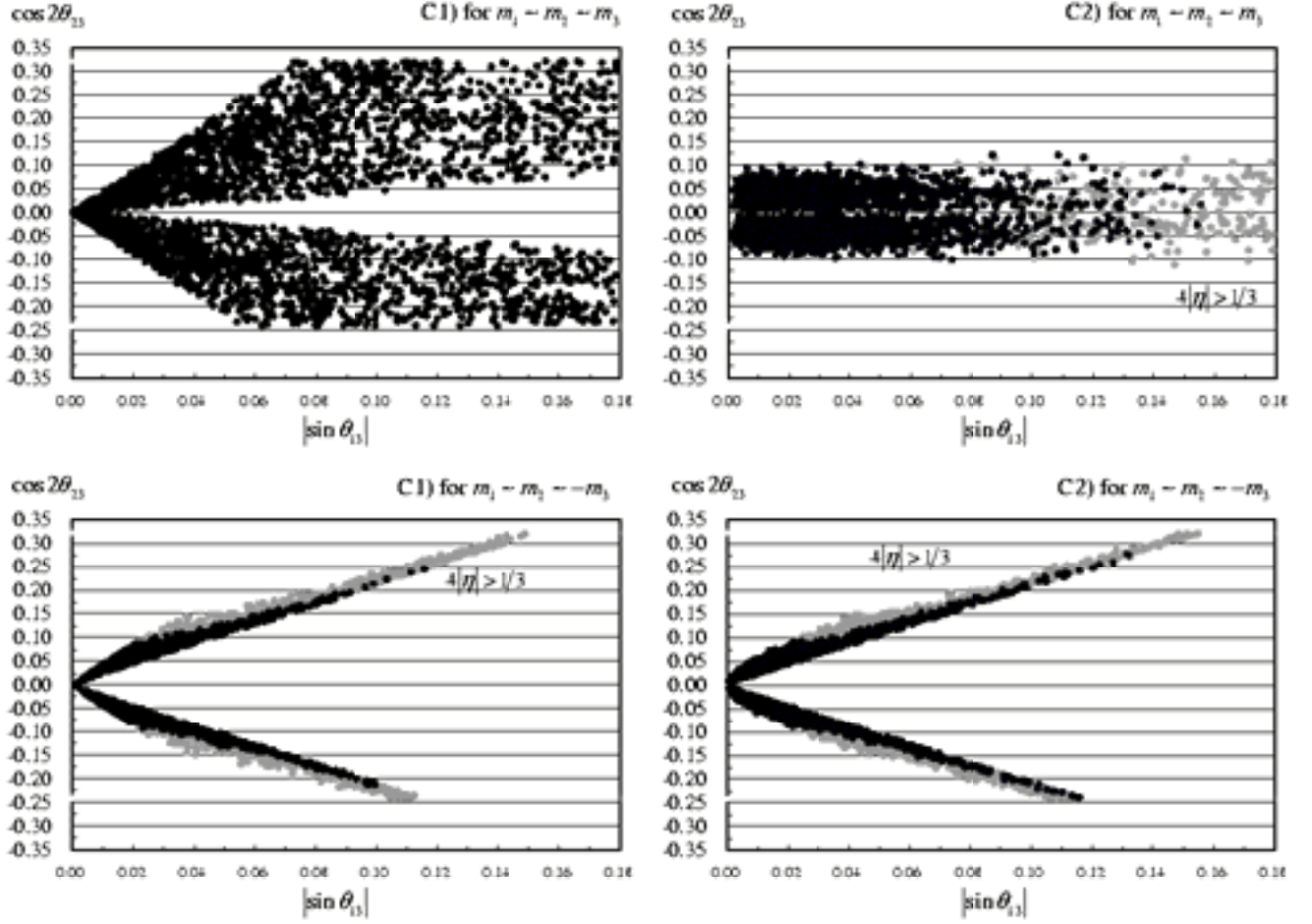


FIG. 14: The same as in FIG.13 but for $\cos 2\theta_{23}$.

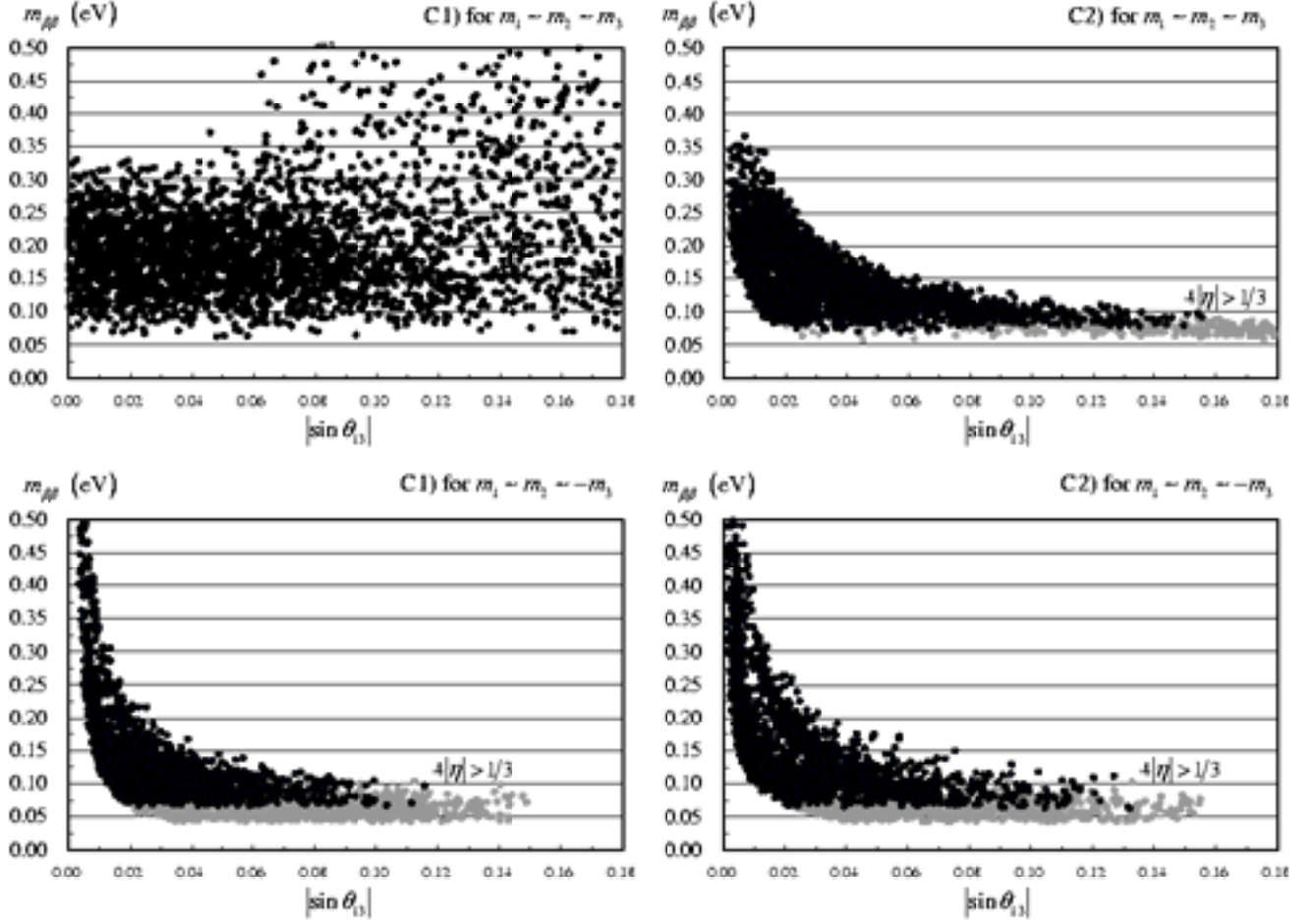


FIG. 15: The same as in FIG.13 but for $m_{\beta\beta}$.